THE STREPTOCOCCUS INVASION LOCUS IN *S. INTERMEDIUS* B196

AN ANALYSIS INTO THE FUNCTIONING OF THE *S. INTERMEDIUS* B196 *STREPTOCOCCUS* INVASION LOCUS

By BRYAN WU, B. SC

A thesis

submitted to the Department of Biochemistry and Biomedical Sciences

and the School of Graduate Studies of McMaster University

in Partial Fulfillment of the Requirements

for the Degree of Master of Science

Descriptive Note

Master of Science (2018) McMaster University
(Biochemistry) Hamilton, Ontario

TITLE: An Analysis into the Functioning of the *S. intermedius* B196 *Streptococcus* Invasion Locus

AUTHOR: Bryan Wu
B. Sc.,
McMaster University, Hamilton, Ontario

SUPERVISOR: Dr. Michael G. Surette

NUMBER OF PAGES: xiv, 78

Lay Abstract

The *Streptococcus* are a group of bacteria known for causing diseases ranging from strep throat to flesh-eating disease; however, many species of *Streptococcus* are usually non-pathogenic, and live in our bodies without causing harm. One group of these bacteria, the *Streptococcus* Anginosus Group (SAG), is commonly found in our mouths and gut and usually cause no harm; however, in some cases it can cause infections. How these organisms switch from being non-pathogenic to pathogenic is unknown, but recently a gene network that appears to play a role in infection, the *Streptococcus* invasion locus (*sil*), was identified in the SAG. This gene network senses the signals released by other bacteria with the network, and only turns on when enough signal is present. The goal of this study is to examine how the system works in the SAG in order to determine how these bacteria coordinate *sil* gene expression.

Abstract

The *Streptococcus* Anginosus Group (SAG) is a group of Gram-positive cocci which require carbon dioxide to grow. They are commensal members of the healthy upper respiratory, gastrointestinal and female urogenital tract; however, they are most commonly known as major pathogens in brain and liver abscesses, forming both mono- and polymicrobial infections. The *Streptococcus* invasion locus (*sil*), first identified as a virulence factor in Group A *Streptococcus* (GAS), has recently been identified in the SAG. The *sil* locus in GAS is a two component quorum-sensing system composed of three operons: *silAB*, coding for a two component system; *silE/D/CR*, coding for an ABC transporter and a signal peptide, and *silC*, which overlaps *silCR* on the opposite strand. The presence of exogenous SilCR activates SilA, which in turn upregulates the transcription of the *silE/D/CR* operon. In the SAG, however, *silCR* and *silED* have distinct promoters, and the SAG *sil* system lacks the *silC* gene. In this study, I examined the transcriptional dynamics of the *sil* system in *S. intermedius* B196. I determined that SilA is the major regulator of the genes in the *sil* system, being one of the first genes of the system to be expressed, and likely upregulates its own transcription. I also found evidence suggesting that, despite having its own promoter, *silCR* transcription may still be driven by the *silED* promoter. I also found evidence that suggests *silED* may be responsible for the export and/or processing of bacteriocins targeting closely related species or strains.

Acknowledgements

No man is an island, and no thesis is completed by a single person. These pages are written from shoulders of giants, and we see far, whether it be a passing word, or a small remark, from which we glean sudden insight; not so much from the height, but rather from the stirring of their wake, the glimpses of the world below from the disturbed clouds, stretching out as far as these eyes can see. As far as these paper wings can fly.

I would like to express thanks to my supervisor, Dr. Michael Surette, for his helpful advice, encouragement, and for taking me on as a graduate student. I may have meandered through the space of possible research questions, but he always was willing discuss my questions, wherever they may be.

My committee members Dr. Brian Coombes and Dr. Nathan Magarvey, for their advice on the direction of my project, and for raising questions that I had not previously considered. It is useful to take a step back to look at the problem from the outside, to see what you are missing.

Michelle Shah and Laura Rossi, for their boundless repository of knowledge that they allowed me to query. Many a time I have interrupted them to ask a question, or a second opinion, and every time they responded with more patience than I probably deserved.

Daphnée Lamarche and Patrick Schenck, for their considerable considerate advice and for serving as a sounding board for discussion and ideas.

Dr. Michelle Mendonca, who initially taught me everything to know about *S. intermedius* B196. There was much to learn, and I am thankful to have a patient and knowledgeable teacher.

Ophélie Quillier and Rachel Szymkiewicz, whose friendship was invaluable. I could have done it without you, but it would have been a much lonelier journey.

And finally, to my family, to whom I apologize for my disappearance. I'm sure they understand.

No man's art - so plainly, see -

Can ask, know, capture symmetry!

Table of Contents

List of Figures

List of Tables

List of Abbreviations and Symbols

Amp	Ampicillin
ABC	ATP-binding cassette
ATP	Adenosine triphosphate
B196	*Streptococcus intermedius* B196
CPS	Counts per second
DNA	Deoxyribonucleic Acid
FRT	Flippase Recognition Target
GAS	Group A *Streptococcus*
GGS	Group G *Streptococcus*
LB	Lysogeny Broth
M505	*Streptococcus constellatus* M505
OD_{600}	Optical Density, 600 nm
NEB	New England Biolabs
PCR	Polymerase Chain Reaction
RNA	Ribonucleic Acid
RT-PCR	Reverse Transcriptase-Polymerase Chain Reaction
SAG	*Streptococcus* Anginosus Group
Spec	Spectinomycin
TCS	Two-Component System
THY	Todd Hewitt Broth with 0.5% Yeast Extract
TOP10F’	*Escherichia coli* TOP10F’

Declaration of Academic Achievement

Bryan Wu designed all experiments and analyzed all results. Dr. Michelle Mendonca created the *S. intermedius* B196Δ*silCR* knockout construct as well as the primers as indicated. Anne-Marie Lacroix created and transformed the *S. intermedius* B196 strains bearing the *luxABCDE* reporter constructs. Dr. Michael Surette provided general advice and aided in the design and conception of all experiments.

Chapter 1: Introduction

1.1. The *Streptococcus* genus

The streptococci are a group of Gram-positive cocci, typically arranged in pairs or chains. They are non-spore-forming, non-motile, facultative anaerobic bacteria that are most often found associated with the mucosal surfaces of animals (Hardie & White, 1997). Streptococci have long been associated with human disease, with the first known medical description of scarlet fever being described by Ingrassia in 1553, which is now known to be caused by the organism *Streptococcus pyogenes* (Ferretti & Köhler, 2016). The first streptococci were isolated by Billroth in 1874 from wound infections, and have since been a major medical focus due to their pathogenic potential (Billroth, 1874; Ferretti & Köhler, 2016).

Early classification of the streptococci was done by observing hemolysis on blood agar plates. In 1919, Brown described the three types of hemolysis patterns in streptococci: “alpha”, a green zone of discolouration (from which the term viridans derives); “beta”, a clear zone of complete hemolysis; and “gamma”, where no zone of hemolysis was observed. In 1933, Lancefield introduced a classification system based off group-specific cell wall antigens, establishing groups A through E. In 1937, Sherman introduced a classification scheme which included the Lancefield antigen, hemolysis and eight other factors, which separated the streptococci into four groups: pyogenic, which were organisms

associated with infection; viridans, organisms from the oral and gastrointestinal tract; lactic, from dairy sources; and enterococcus, from fecal origin. In 1987, the latter two groups were reclassified into the *Lactococcus* and *Enterococcus* genera respectively, using genetic approaches amongst other methods (Schleifer & Kilpper-Bälz, 1987).

Using 16s rRNA comparative sequence analysis, the streptococci are currently classified into six phylogenetic groups: pyogenic, anginosus, mitis, salivarius, bovis, and mutans; the latter five of which previously belonged to the viridans group (Kawamura *et al.*, 1995).

1.1.1. The *Streptococcus* Anginosus Group

The *Streptococcus* Anginosus Group (SAG) is composed of three phylogenetically closely-related members: *S. anginosus*, *S. intermedius*, and *S. constellatus*. Common characteristics shared among the SAG members are small colony sizes (<0.5 mm), a slower growth rate, a caramel odour due to diacetyl production, and a requirement of carbon dioxide for growth. Despite their relatedness, these organisms demonstrate great phenotypic heterogeneity, varying in Lancefield grouping (A, C, G, F, non-groupable) and hemolysis pattern on blood agar (alpha, beta, gamma), among others characteristics (Piscitelli *et al*., 1992).

Members of the SAG are found at various mucosal membranes of healthy individuals, including the upper respiratory, gastrointestinal and urogenital tracts, although they are also clinically known for being associated with pyogenic infections such as brain and liver abscesses, pleural empyemas, periodontal disease, endocarditis, meningitis, as well as skin and soft tissue infections (Siegman-Igra & Schwartz, 2012). Many of these infections are secondary to oral or abdominal trauma, which may allow these organisms to travel to the sterile body sites (Gossling, 1988). SAG members are also known to cause polymicrobial abscesses with other anaerobic organisms and Gram-negative pathogens (Piscitelli *et al*., 1992, Siegman-Igra & Schwartz, 2012).

1.2. Two-component systems

Two-component systems (TCSs) are a common mechanism for bacteria to sense changes in the environment, allowing them to adapt and respond to their surroundings. Found abundantly in bacteria, and less commonly in eukaryotes, TCSs control a wide variety of processes, including chemotaxis, metabolism, osmoregulation and virulence (West & Stock, 2001). The prototypical TCS is composed of two components: a histidine kinase and a response regulator, where an activated histidine kinase changes the phosphorylation state of the response regulator. Despite their name, many TCSs have other auxiliary regulatory proteins

that modify the phosphorylation state of the response regulator (West & Stock, 2001; Bourret & Silversmith, 2010).

Histidine kinases are typically homodimeric transmembrane proteins, and function as cellular receptors with both kinase and phosphatase activity. Upon the binding of a ligand to the N-terminal extracellular domain of the histidine kinase, the protein undergoes a conformational change, changing the kinase/phosphatase activity ratio of the enzyme. The prototypical histidine kinase increases the kinase/phosphatase activity upon ligand binding, but some are known to decrease the ratio (Raivio & Silhavy, 1997). In the typical model, the conformational change activates the ATP-binding kinase domain, which transfers the phosphate group of an ATP molecule to a histidine residue on the histidine phosphotransferase domain, resulting in autophosphorylation. The phosphate group is then transferred to the receiver domain of the response regulator (Figure 1.1, West & Stock, 2001).

Response regulators usually consist of two domains: the receiver domain and the effector domain. The receiver domain catalyzes the transfer of the phosphate group from the histidine phosphotransferase domain, and, upon phosphorylation, often results in conformational changes which activate the effector domain (West & Stock, 2001). A number of effector domain families exist, the majority of which are transcriptional regulators that bind DNA, although other enzymatic and RNA-binding domains exist (Galperin, 2006).

An example family of transcriptional regulators is the LytTR family of response regulators, which are commonly found regulating virulence in plant and human pathogenic bacteria (Behr et al., 2016). The LytTR family binds to two direct or inverted repeats 9-11 nucleotides in length, separated by an 11-13 nucleotide spacer, in the major groove of DNA via a potential winged helix-turn-helix domain. DNA-binding specificity is mediated by a highly variable loop region in the effector domain, and occurs as a two-step process: the response regulator initially binds to one of the repeats, which dimerizes and aids in the binding of its partner to the second repeat. This is thought to result in the bending of the bound DNA, and serves as the protein interface in the recruitment of RNA polymerase. It is thought that the dissociation of the response regulator from the second repeat initiates promoter clearance, serving as a tight control mechanism for gene expression (Behr et al., 2016).

The receiver domain also has the ability to change its own phosphorylation state. Autophosphorylation has been shown with small molecule donors in the absence of the histidine kinase due to the catalytic receiver domains of response regulators. Auto-dephosphorylation limits the active lifetime of the response regulator, and occurs intrinsically as well as through interactions with other proteins (West & Stock, 2001).

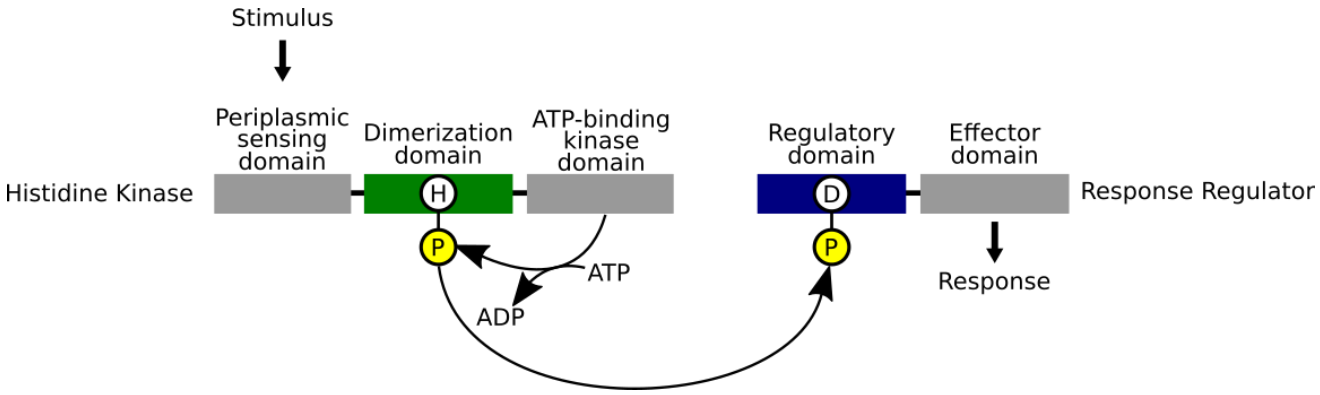

Figure 1.1: A typical two-component phosphotransfer system. The system consists of a dimeric transmembrane sensor histidine kinase and a cytoplasmic response regulator. Upon sensing a signal from the periplasmic sensing domain, the ATP-binding kinase domain phosphorylates a histidine residue (H) in the dimerization domain, which is then transferred to an aspartate residue of the regulatory domain of the response regulator, which activates the effector domain, resulting in a downstream response. Figure adapted from West & Stock (2001)

There is evidence *in vitro* that histidine kinases can cross-phosphorylate the response regulators of other systems, resulting in crosstalk between different two-component systems. *In vivo*, however, crosstalk between two-component systems is rare (Laub & Goulian, 2007), and is primarily due to the high specificity of histidine kinases for their cognate response regulators (West & Stock, 2001).

1.2.1. Quorum-sensing systems

Cell-to-cell signalling in bacteria is known as quorum-sensing. This signalling is triggered by the presence of signal molecules known as autoinducers. As these bacteria produce their own signals, the concentration of the autoinducer is often a proxy for cell density (Belotserkovsky *et al*., 2009). The individual members typically express the autoinducer at low concentrations, and when the local concentration of extracellular signalling molecule reaches a certain threshold, the interaction of the molecule with a receptor protein results in a synchronized change in gene expression in the population (Abisado *et al.*, 2018). As the autoinducer is expressed into the extracellular environment, the system is also impacted by environmental conditions, ranging from pH, temperature, and the presence of other bacteria, some of which have the ability to degrade autoinducers or release inhibitors, making quorum-sensing systems a sensor by

which bacteria detect changes in the environment (Wisniewski-Dyé & Boyer, 2009).

Quorum-sensing systems are also often tightly controlled by regulators responding to environmental conditions, ranging from nutrient availability to cell stress and energy state. Quorum-sensing systems are also known to regulate other quorum-sensing systems in series, creating a hierarchical network that is believed to play a role in the temporal order of expression (Wisniewski-Dyé & Boyer, 2009). In some cases, the expression of the signal is also controlled by the system itself, resulting in a positive feedback loop leading to an abrupt activation of the system. Quorum-sensing systems are known to regulate a large variety of different genes, such as those involved in light generation, competence stimulation, virulence, bacteriocin production, and biofilm formation (Abisado *et al.*, 2018).

The prototypical Gram-negative quorum-sensing system is the acyl-homoserine lactone quorum-sensing system from *Vibrio fischeri* which drives bioluminescence (Figure 1.2). *N*-3-oxo-hexanoyl-homoserine lactone synthesis is driven by the gene *LuxI*, and diffuses through the cell membrane into the environment. The signal molecule binds specifically to the transcription factor LuxR, which activates the downstream expression of the *luxCDABEG* operon responsible for bioluminescence, along with other downstream genes (Abisado *et al*, 2018).

Some Gram-positive and Gram-negative bacterial species have peptide-based quorum-sensing systems (Lyon & Novick, 2003), which use peptide-based signalling molecules rather than small molecules. The signal peptide is synthesized as a propeptide, which is processed and secreted by an ATP-dependent transporter. Once reaching a critical threshold outside of the cell, the mature signal peptide is detected by a two-component system, which activates the intracellular response pathway (Lyon & Novick, 2003).

1.3. The *Streptococcus* invasion locus

The *Streptococcus* invasion locus (*sil*) is a quorum-sensing system associated with virulence and bacteriocin production. First identified in Group A *Streptococcus* (GAS), the core system is composed of six genes in three operons, the first coding for a two-component sensor/response regulator (*silAB*), and the second coding for a signal peptide (*silCR*), and an ATP-binding cassette (ABC) transporter (*silED*). A third operon lies on the opposite strand of *silCR* and codes for *silC*, which competes with *silCR* for transcription. In the GAS, the SilCR propeptide is thought to be cleaved at a double-glycine leader and exported by SilDE, and the mature SilCR peptide is thought to activate SilAB, which upregulates the expression of SilCR and SilDE, along with other downstream genes, resulting in an autoinduction loop (Eran et al., 2007).

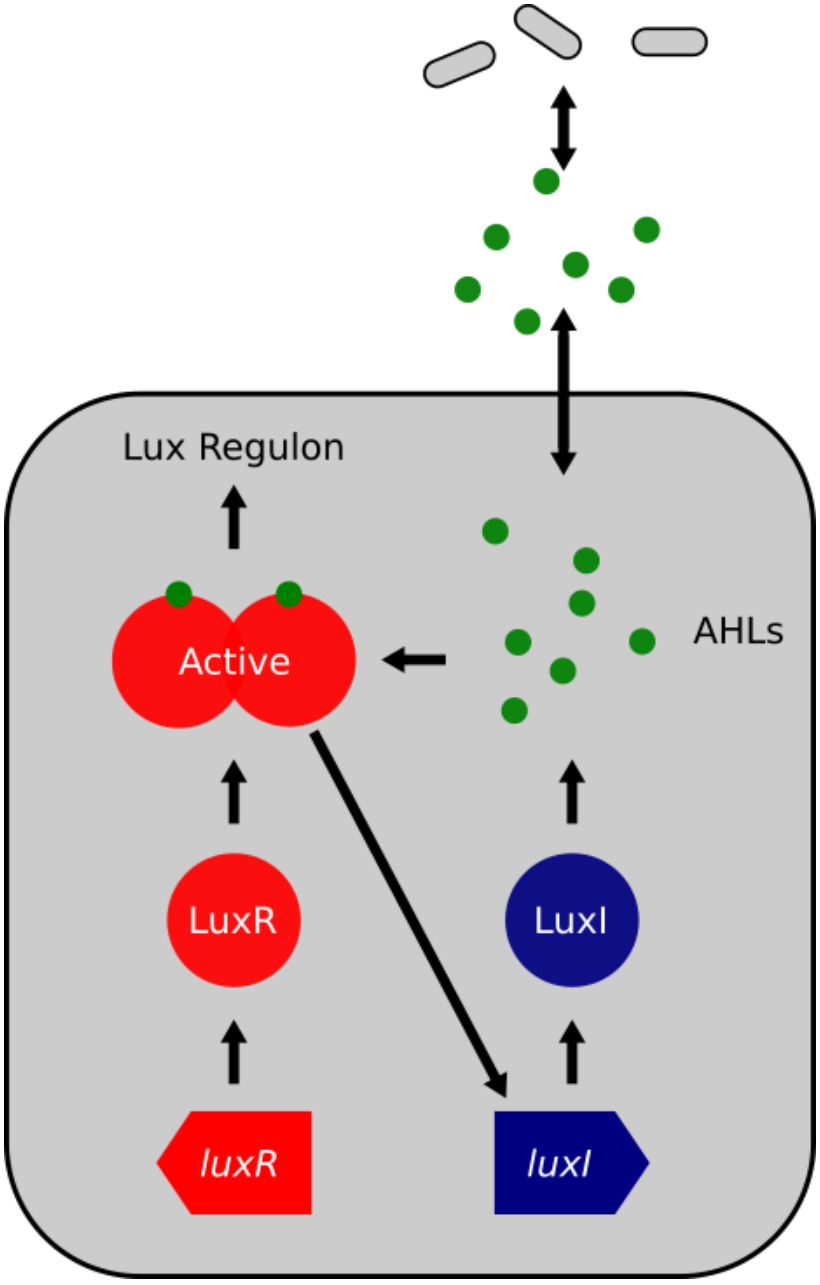

Figure 1.2: N-acyl homoserine lactone (AHL) quorum-sensing system in *Vibrio fischeri*. AHLs (green circles) are sensed by the LuxR family of transcription factors, and binding results in a conformational change resulting in the activation of LuxR. LuxR drives the expression of the LuxI AHL synthases, resulting in a positive feedback loop. As AHLs are able to diffuse into the environment, AHLs produced by other bacteria can be sensed as well. Figure adapted from Abisado *et al.* (2018).

1.3.1. The identification of the *sil* locus in *Streptococcus*

The *sil* locus was initially identified by Hidalgo-Grass *et al.* (2002) through signature-tagged mutagenesis in GAS strain JS95 and is associated with a downstream bacteriocin locus (Figure 1.3). One mutant was identified to survive in the skin but failed to spread to the spleen, and the region of insertion was designated the *sil* locus (Hidalgo-Grass *et al.*, 2002), as disruption of the locus reduced the ability of the bacteria to invade and cause lethal infection.

Both the deletion of *silC* and the inactivation of *silB* through mutagenesis decreased mortality in mice; however, co-injection of the *silC* knockout with an avirulent mutant of JS95 rescued mortality in mice, whereas injecting the two mutants at different sites raised lethality only slightly. (Hidalgo-Grass *et al.*, 2002).

In Eran *et al.* (2007), the operon structure was confirmed by RT-PCR, and the addition of synthetic SilCR peptide increased the expression of the *silE/D/CR* operon in early and late logarithmic growth, but not at early stationary phase, in a SilCR concentration-dependent manner. Additionally, the addition of SilCR slightly upregulated the expression of *silA* independent of growth phase. *silA* and *silB* mutants did not respond to the addition of synthetic SilCR.

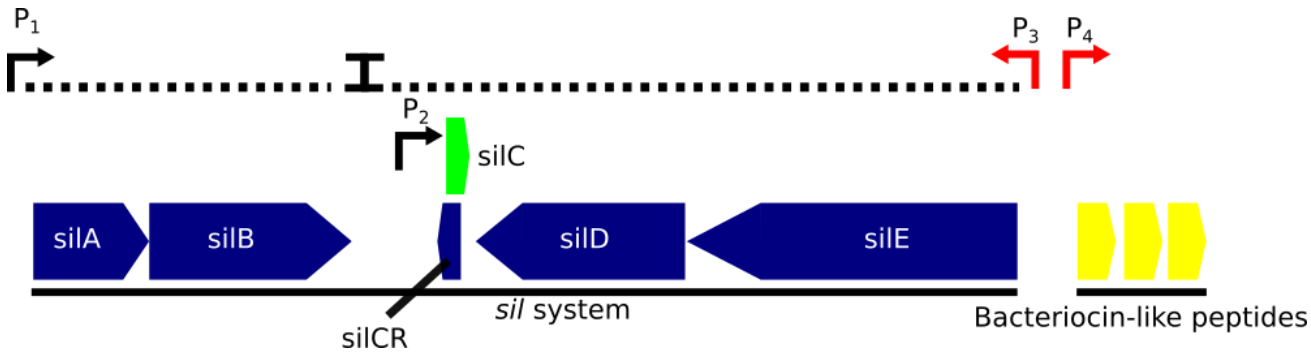

Figure 1.3: The *sil* system in Group A *Streptococcus*. The *sil* system in GAS consists of three operons: the *silAB* two-component system, the *silC* transcript, and the *silE/D/CR*, transcript, coding for both the *silED* ABC transporter and the *silCR* signal peptide, and an associated downstream locus containing bacteriocin-like peptides. Promoters 4 and 3 (red) are strongly upregulated by the presence of exogenous SilCR. Figure adapted from Belotserkovsky *et al.* (2009).

Eran *et al.* (2007) also found that the ongoing transcription of *silCR* suppresses the transcription of *silC* on the opposite strand, and that the *sil* system regulates the expression of downstream bacteriocins, which may play a role in microbial competition.

In Hidalgo-Grass *et al.* (2004), they demonstrated that the addition of SilCR increases mouse survivability by abrogating the expression of the serine peptidase *scpC*; however, Salim *et al.* (2008) showed that the addition of SilCR increases the expression of various virulence factors, including the cytolysin streptolysin C and iron acquisition, in a strain of GAS lacking the *sil* system, indicating that the SilCR peptide may interact with other TCSs in GAS to increase virulence.

One difficultly of linking the *sil* locus with virulence in GAS is that many strains do not contain functional *sil* systems. Plainvert *et al*. (2014) showed that only 9% of 637 clinical GAS samples had a predicted functional *sil* system. In the JS95 strain, the start codon of *silCR* is mutated to AUA, and antibody testing could not detect the presence of SilCR (Eran *et al.*, 2007).

The *sil* system was later identified in Group G *Streptococcus* (GGS), and testing showed that cross-recognition occurs between the SilCR produced by GGS and GAS. Additionally, the SilA-binding site was identified as a pair of imperfect direct 10-bp repeats separated by an 11-bp spacer, which follows from the

prediction that SilA is a LytTR-family response regulator (Belotserkovsky *et al.*, 2009).

Michael-Gayego *et al.* (2013) identified the *sil* locus in 25% of clinical GAS isolates and 82% of clinical Group G *Streptococcus* (GGS) isolates, and found that mice immunized against SilCR developed more severe infections of GGS.

1.3.2. The *sil* Locus in the *Streptococcus* Anginosus Group

Mendonca *et al.* (2016) identified the *sil* locus in 42/44 *Streptococcus* Anginosus Group strains, spread among all three species, which range from 68.0% to 90.3% amino acid sequence identity to the GAS *sil* system genes (Figure 1.5). Of major interest is that the *sil* system in SAG is predicted to lack *silC*, suggesting that the *sil* system in SAG is lacking the negative regulation that *silC* affords. Additionally, there is a *sil*-associated accessory locus different from the one identified in GAS, and has been shown through genomic analysis to be a highly variable region within the SAG.

SilA-binding sites in the SAG member *S. intermedius* B196 were predicted upstream of *silCR*, *silE*, a predicted CAAX protease, and a predicted protein that contains a thioredoxin-like domain, as well as upstream of three co-occurring sets

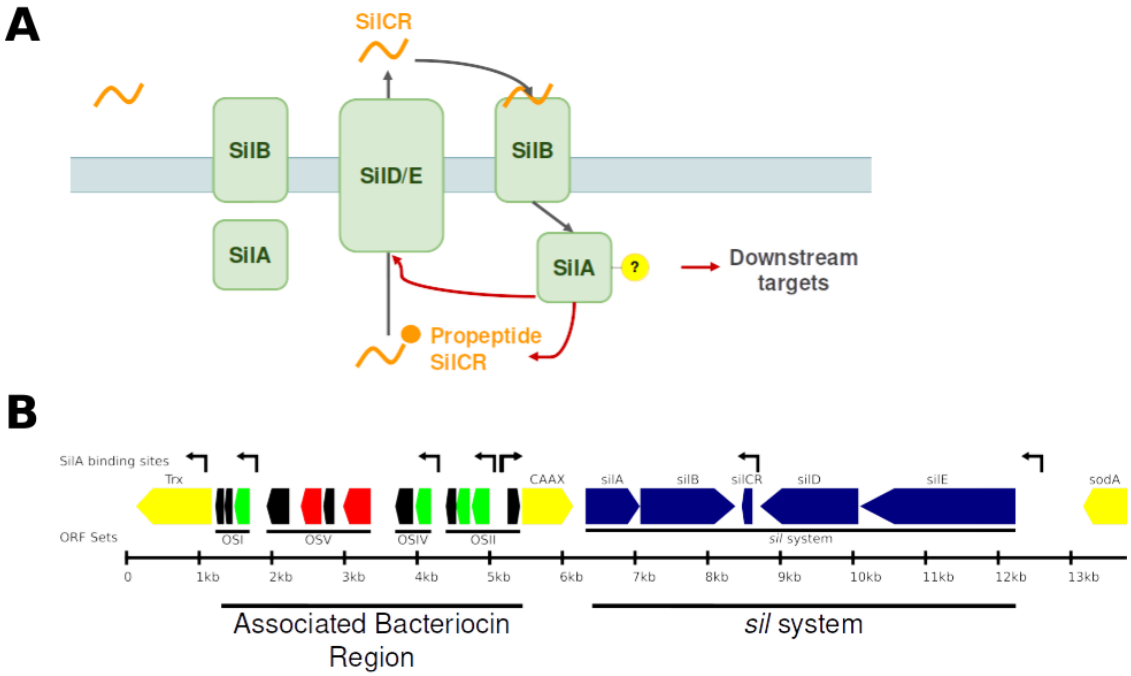

Figure 1.5: The *sil* system in *S. intermedius* B196. I hypothesize that the propeptide SilCR is processed and exported by the ABC transporter SilDE. Exogenous mature SilCR peptide binds to SilB, which modifies the phosphorylation state of SilA, activating the response regulator to upregulate the expression of *silCR* and *silED*, in addition to other downstream targets (A). The *sil* system in B196 is downstream of an associated bacteriocin region (B). SilA-binding sites have been predicted upstream of a number of genes in the *sil* locus (black arrows) and associated bacteriocin region. OSI-IV indicate open reading frame sets that were found to be co-associated in various SAG strains. Adapted from Mendonca *et al.* (2016).

of open reading frames in the upstream accessory region. A consensus sequence for SilA-binding in SAG was predicted as ACCATTCAGG-11bp-ACCATTTAGG.

Mendonca *et al.* demonstrated that *S. intermedius* B196 inhibits the growth of SAG member *S. constellatus* M505, which is lacking the *sil* locus, in a *silCR*-dependent manner. A deletion of *silCR* in B196 abrogates the inhibition of M505, and the addition of synthetic SilCR peptide rescues inhibition in a dose-dependent manner. Real-time RT-PCR analysis show that *silE* expression is downregulated in Δ*silCR* colonies (Mendonca *et al.*, 2016).

Additionally, among the strains analyzed, two distinct SilCR peptides were identified, each with an associated variant SilB histidine kinase. Testing the two SilCR variants on Δ*silCR* showed that the non-cognate SilCR requires higher concentrations to elicit a response (Mendonca *et al.*, 2016).

1.4. Objectives and Hypothesis

The recent identification of the *sil* system and its high prevalence in the SAG is of interest due to its putative function in regulating the expression of bacteriocins, especially as a means of interaction between the bacteria in polymicrobial infections. The differences between the systems in SAG and GAS is also of interest, specifically, the presence of predicted SilA-binding sites upstream of the *silCR* gene, and the lack of a *silC* gene. No functional analysis of the system in SAG has yet been done.

Building off previous work performed into the *sil* system, I hypothesize that the sil locus in *S. intermedius* B196 functions in an autoregulatory manner, where *silAB* codes for the response regulator/histidine kinase pair, that when activated by SilCR, induces the expression of *silCR* and *silED*. SilCR is then exported into the environment by SilDE, where it can activate SilAB, leading to a positive feedback loop and nonlinear expression dynamics.

In order to test this hypothesis, two objectives were undertaken:

1. To investigate the promoter activity in the *sil* locus of *S. intermedius* B196 over time. By capturing the temporal activity of the promoters in the *sil* system, it will be possible to model the interaction between the genes, and determine the effect of autoinduction on the activation of the *sil* system genes.

2. To determine the impact of gene deletions on the transcription patterns within the *sil* system. Examining how *sil* gene deletions affect the transcription of the remaining *sil* system genes, as well as the functioning of the system as a whole, can provide information about the interaction network of genes in the *sil* system.

Chapter 2: Materials and Methods

2.1. Bacterial strains, growth conditions and plasmids

Streptococcus anginosus Group (SAG) strains *S. intermedius* B196 and *S. constellatus* M505 were used in this study. All SAG strains, unless otherwise stated, were grown in Todd-Hewitt broth (Bacto) supplemented with 0.5% yeast extract (THY; Bacto). *Streptococcus intermedius* B196 was incubated in 5% CO_2 at 37°C, whereas *S. constellatus* M505 was incubated anaerobically (5% CO_2, 5% H_2, 90% N_2) at 37°C. Bacterial stocks were maintained at -80°C in 10% skim milk.

One Shot™ TOP10F' Chemically Competent *Escherichia coli* (Thermo Fisher) was used during cloning. *E. coli* cells were grown in Luria-Bertani (LB) medium aerobically at 37°C. *E. coli* stocks were maintained at -80°C in 20% glycerol.

The bacterial strains and plasmids that were used in study are described in Table 2.1. Primers used in this study are described in Table 2.2.

Antibiotic concentrations for selection were as follows: spectinomycin (Spec), 75-100 µg/mL and ampicillin (Amp), 100 µg/mL.

2.2. The impact of Tween 80 on aerobic growth of *S. intermedius* B196.

2.2.1. Aerobic growth of *S. intermedius* B196 in 96-well plates

Streptococcus intermedius B196 transformed with *luxABCDE* reporter plasmids for the promoters upstream of *silA*, *silCR* and *silE* (created by Anne-

Marie Lacroix, a previous member of the lab) were cultured overnight in THY containing 75 µg/mL Spec. Overnight cultures were diluted to 0.1 OD_{600}, and 15 µL was used to inoculate wells on a 96-well plate containing 135 µL fresh THY containing 75 µg/mL spectinomycin, and 0.2% Tween 80 in some experimental conditions. 50 µL of filter-sterilized mineral oil was overlaid over each well to reduce evaporation, gas exchange, and to prevent oxidative stress. Cells were incubated aerobically in a BioTek Synergy H1 Hybrid Multi-Mode Reader at 37°C, with OD_{600} measurements taken every 5 minutes. Plates were double-orbitally shaken at 180 rpm for 1 minute prior to each read.

2.2.2. Polylysine coverslip preparation

Polylysine was used to fix the cells to the glass coverslip so that all the cells would be on a single plane of focus. Glass coverslips were each covered in 1 mL 100 µg/mL poly-L-lysine (Sigma-Aldrich). The coverslips were incubated at room temperature for 5 minutes, then washed with 0.85% saline solution. Coverslips were left to dry prior to use.

2.2.3. LIVE/DEAD staining

Streptococcus intermedius B196 was grown overnight under three environmental conditions (anaerobically, 5% CO_2, and aerobically) and two media conditions (THY and THY + 0.2% Tween 80) at 37°C, and stained using the

LIVE/DEAD *Bac*Light Bacterial Viability Kit (ThermoFisher Scientific). Cells were then pelleted, washed and resuspended in 0.85% saline solution. 5 µL of a 1/10 dilution in 0.85% saline solution was incubated on polylysine-coated coverslip for 20 minutes at room temperature. The polylysine-coated coverslips were then washed with 0.85% saline solution prior to visualization under a fluorescence microscope (Leica DM4000 B LED) at 480/520 nm and 540/630 nm.

2.3. Construction of Δ*silAB* and Δ*silED S. intermedius* B196 strains.

2.3.1. Construction of a flippase recognition target (FRT)-flanked spectinomycin resistance cassette.

Using PCR, the spectinomycin resistance cassette was amplified from the plasmid pDL278 using the primers SpecF and SpecR, which were derived from Mendonca *et al.* (2016). FRT sites were amplified from the plasmid pKD4, using the primer pairs FRTupF/FRTupR and FRTdownF/FRTdownR. The spectinomycin resistance cassette and the downstream FRT site were digested with *Xho*I and ligated with T7 DNA ligase to form the Spec-FRT ligation. The Spec-FRT ligation was amplified using primers SpecF and FRTdownR and purified with the PureLink Gel Extraction Kit (Life Technologies). The Spec-FRT ligation and the plasmid pUC19 were digested using *Bam*HI and *Sal*I and ligated. The resulting ligation was transformed into TOP10F' Chemically Competent *E. coli* (Thermo Fisher), and transformants were selected for by plating onto THY agar containing 75 µg/mL

spectinomycin. The resulting pSF vector was purified using PureLink Quick Plasmid Miniprep Kit (Invitrogen). pSF and the upstream FRT site were then digested using *Sac*I and *Bam*HI, and ligated. The ligation product was transformed into TOPF' and plated on THY agar with 75 µg/mL spectinomycin. The resulting pFSF vector was purified using the PureLink Quick Plasmid Miniprep Kit (Invitrogen) and confirmed with gel electrophoresis and sequencing the insertion of the upstream FRT site.

2.3.2. Deleting *silAB* and *silED* from *S. intermedius B196*.

To delete *silAB* and *silED*, genomic DNA from *S. intermedius* B196 was extracted using the Wizard Genomic DNA Purification Kit (Promega). The flanking regions (1 kb ± 100 bp) of each operon were amplified from the genomic DNA using the primer pairs found in Table 2.2. The upstream flanking region was inserted first, digesting the upstream flanking region and pFSF with *Eco*RI and *Sac*I. The pFSF digest was treated with shrimp alkaline phosphatase (NEB), and the two digests were ligated and transformed into TOPF'. The resulting transformation was plated on THY agar with 75 µg/mL spectinomycin. Plasmids were purified and verified by digesting with *Eco*RI and *Sac*I.

The downstream flanking regions were inserted using a similar protocol, using the restriction enzymes *Sal*I and *Sph*I instead.

Plasmids with both up and downstream flanking regions were digested using *Eco*RI and *Sph*I, and purified using the DNA Clean and Concentrator kit (Zymo Research). Following a transformation protocol developed by former lab member Anne-Marie Lacroix (Lacroix, 2014), overnight cultures of *S. intermedius* B196 were diluted 1/1000, and incubated for 2 hours at 37°C in 5% CO_2. 1 µg of digested plasmid was added to 500 µL of culture along with 200 ng/mL of B196 competence-stimulating peptide, and was left to incubate for an hour. The knockout strains were obtained via double crossover event resulting in the replacement of *silAB*, *silCR*, and *silED* with the FRT-flanked spectinomycin cassette. Successful double recombinants were selected for by plating the cells on THY agar with 75 µg/mL spectinomycin.

2.3.3. Verification of B196Δ*silAB* and B196Δ*silED.*

To verify proper recombination has occurred, I extracted genomic DNA from the knockout strains using the Wizard Genomic DNA Purification Kit (Promega), and amplified the genomic DNA using the primer ORF14_checkF, which lies outside of the *sil* system, paired with primers FRTupF and FRTupR. Products of proper length were obtained for both Δ*silAB* and Δ*silED*, indicating proper recombination for both knockouts.

2.4. *Streptococcus intermedius* B196 inhibition assays against *S. constellatus* M505.

2.4.1. Bacteriocin activity assays.

To evaluate the impact of the various *sil* system knockouts on the SilCR-dependent *S. intermedius* B196 killing of *S. constellatus* M505, I adapted top-overlay experiments from Mendonca *et al.* (2016). 5 µL of overnight cultures of *S. intermedius* B196, the knockout strains B196ΔFSF*silAB,* B196ΔFSF*silED*, and the *S. intermedius* B196Δ*silCR* knockout strain generated by Mendonca *et al.* (2016) were plated on THY agar and grown for 2 days at 37°C in 5% CO_2. Under some experimental conditions, 200 ng of synthetic SilCR peptide (from RS synthesis) was spotted on the surface of the colony. 100 µL of overnight *S. constellatus* M505 THY cultures were then mixed with 5 mL of molten 1.5% THY agar, inverted three times, and poured over the plates with the *S. intermedius* spots. Plates were incubated for 2 days at 5% CO_2 at 37°C.

2.5. Promoter activity of *sil* system genes over time in *S. intermedius* B196.

2.5.1. Measurement of *sil* system promoter activity

Streptococcus intermedius B196 transformed with reporter plasmids were cultured in THY containing 100 µg/mL spectinomycin in 5% CO_2 at 37°C to 0.4 OD_{600} before being placed on ice. Once all cultures had reached 0.4 OD_{600}, 100 µL

of each culture was used to inoculate 10 mL of THY containing 100 µg/mL spectinomycin in triplicate and incubated in 5% CO2 at 37°C. Luminescence and OD_{600} measurements were taken from 200 µL samples every 30 minutes to 1 hour starting at 4 hours of growth.

For the three experiments done on one day, three colonies of B196 containing reporter plasmids were selected from the same plate and inoculated into 3 mL THY containing 100 µg/mL spectinomycin, and grown overnight in 5% CO_2 at 37°C. Overnight cultures were diluted to 0.1 OD_{600}, and 100 µL was used to inoculate 10 mL of THY containing 100 µg/mL spectinomycin in triplicate. Growth and measurements were done as above.

2.5.2. Promoter activity analysis

In order to calculate the time point of maximal growth, growth curves were fitted to a sigmoid function of the expression

$$y(t) = a + \frac{b - a}{1 + e^{-c(t-d)}}$$

using the non-linear least squares approximation in R. Both growth curves and expression curves were then shifted by *d* to align the growth curves to maximal growth rate. Normalized luminescence was generated by dividing the measured luminescence by the maximal luminescence.

OD_{600} and time before maximal growth at 10% maximal luminescence were linearly interpolated from the two closest data points.

Changes in variability were compared using a two-tailed *F*-test of equality of variances, which assumes that the population follows the normal distribution. Multiple tests were done using a one-way ANOVA, and multiple test corrections were done using the Holm-Bonferroni method (Holm, 1979).

2.6. Real-time RT-PCR

2.6.1. RNA Extraction

Cultures of *S. intermedius* B196 and knockout strains were grown to 0.2 OD_{600}, and 100 µL of diluted culture was then used to inoculate 10 mL of THY containing 100 µg/mL spectinomycin. Cultures were incubated in 5% CO_2 at 37°C, and 200 µL was sampled every hour starting at 4 hours to measure OD_{600}. Once OD_{600} reached 0.3, the culture was split into two 3 mL cultures. Synthetic SilCR peptide was added to a final concentration of 50 nM to one of the two cultures. Both cultures were incubated in 5% CO_2 at 37°C for 30 minutes, and both cultures were spun down and decanted. RNA extraction was carried out with TRIzol reagent (Invitrogen) in combination with column purification using the Qiagen RNeasy Kit, following the on-column DNAse digestion step.

2.6.2. cDNA generation and real-time RT-PCR

cDNA was generated from 10 µL of RNA using the Superscript III First-Strand Synthesis System (Invitrogen) following the manufacturer's instructions.

Random hexamer primers were used for the conversion of RNA to DNA, and samples were stored at -20°C. The genes selected for the study included the *sil* system component genes *silA*, *silCR*, and *silE*, as well *rpoB* as a reference gene. Primers for these genes can be found in Table 2.2.

Real-time PCR reactions were carried out in a CFX96 Real-time PCR machine (Biorad). Primers were validated using a thermal gradient and 55°C was determined to be sufficient for all genes. For the samples tested, 20 µL reactions were performed in triplicate using SsoFast Evagreen Supermix (Bio-Rad), 1 µL cDNA and 500 nM of primer. Appropriate no template controls and no reverse transcriptase controls were performed and showed either no amplification or were >5 Cq above the target sequences. Gene expression relative to the wild type was calculated using the delta delta Cq method. Gene expression was normalized to *rpoB* expression.

2.7. Genomic analysis

2.7.1. Promoter prediction in the *S. intermedius* B196 *sil* system

The software BPROM (Solovyev & Salamov, 2011) was used to predict σ^{70} promoter sites 400 bp upstream and downstream of predicted genes in the B196 *sil* system.

2.7.2. Rho-independent terminator prediction in the *S. intermedius* B196 *sil* system

The software ARNold (Naville *et al.*, 2011) was used to predict Rho-independent terminators across the entire B196 *sil* system.

Table 2.1: Bacterial strains and plasmids used in this study

Strain or plasmid	Relevant characteristics	Source or reference
Strains		
E. coli TOP10F'	Cloning strain, *TetR*	Invitrogen
S. constellatus M505	Wild type	Kaiser *et al.*, 2014
S. intermedius B196	Wild type	Olson *et al.*, 2013
S. intermedius B196ΔFSF*silAB*	*silAB* knockout, FRT-flanked *SpecR*	This study
S. intermedius B196ΔFSF*silCR*	*silCR* knockout, FRT-flanked *SpecR*	This study
S. intermedius B196ΔFSF*silED*	*silED* knockout, FRT-flanked *SpecR*	This study
S. intermedius B196Δ*silCR*	*silCR* knockout, *SpecR*	Mendonca *et al.*, 2016
Plasmids		
pUC19	*E. coli* cloning vector, *AmpR*	
pDL278	*E. coli-Streptococcus* shuttle vector, *SpecR*	LeBlanc *et al*., 1992
pKD4	*E. coli* FRT-flanked kanamycin resistance cassette, *AmpR*	Datsenko & Wanner, 2000
pSF	pUC19 harboring a partially FRT-flanked *SpecR*	This study
pFSF	pUC19 harboring an FRT-flanked *SpecR*	This study
pFSF-silAB	pUC19 harboring a B196 *silAB* knockout construct	This study

Table 2.2: Primers used in this study

Primers	Oligonucleotide sequence (5′ → 3′)	Source
Real-time PCR		
silAB_FWD	ATCTGAGAAAGGAAGCCATCAG	This study
silAB_REV	GCATAAGGATCTATCTCGCGTATC	This study
silCR_FWD	ACAAACATTGGATCATTTTCGTACACTCAC	Mendonca *et al.*, 2016
silCR_REV	AGCCTAATGTATTATTTGAATCTCCCTTTGTTAAAC	Mendonca *et al.*, 2016
silED_FWD	TGATGCTCTCGCTTCTACAATAC	This study
silED_REV	GCAAGCAGAGTGAGGAAGAA	This study
rpoB_FWD	GGCCGTGTGGATGATATTGA	This study
rpoB_REV	CATTACGCTCCATCCGAGAAA	This study
ΔsilAB		
silABupF	AAAA**GAATTC**GTGAATTTCCACCCCCACCA	This study
silABupR	AAAA**GAGCTC**AAAAGGATTGGAAGTTCACAAGAA	This study
silABdownF	AAAA**GTCGAC**TCGTACATATACAAATAACCTCATCGC	This study
silABdownR	AAAA**GCATGC**AAGCTGGTACTGGAACTGCG	This study
ΔsilED		
silEDupF	AAAA**GAATTC**ACAAAGCAGCGAAATAAGACAACA	This study
silEDupR	AAAA**GAGCTC**TTTACGTAGGTAATAGTAGACACGT	This study
silEDdownF	AAAA**GTCGAC**AGGACAAAATCACTACCATTTAAGATT	This study

silEDdownR	AAAA**GCATGC**TCGGAGCTTTCGGCATGATT	This study
Spectinomycin		
SpecF	AAAAA**GGATCC**GACGAAGAGGATGAAGAGG	Mendonca *et al.*, 2016
SpecR	AAAAA**CTCGAG**CCCAAATATTAAATAATAAAAC	Mendonca *et al.*, 2016
FRT		
FRTupF	AAAA**GAGCTC**GCCCACCCCAGCTTCAAAAG	This study
FRTupR	AAAA**GGATCC**AGCCATGGTCCATATGAATATCCT	This study
FRTdownF	AAAA**CTCGAG**GCCCACCCCAGCTTCAAAAG	This study
FRTdownR	AAAA**GTCGAC**AGCCATGGTCCATATGAATATCCT	This study
Verification		
ORF14_checkF	CGAGCTATAACGGTGGTGGA	This study

Bold sequences indicate restriction endonuclease sites introduced into the primers for the purpose of cloning the amplified product.

Chapter 3: Results

3.1. Tween 80 increases growth of *S. intermedius* B196 under aerobic conditions without CO_2.

Streptococcus Anginosus Group members have been shown to require CO_2 for growth. Tween 80, also known as polysorbate 80, is a non-ionic surfactant and emulsifier that has been shown to aid in the growth in liquid culture of streptococcal species in the absence of CO_2 (Deibel & Niven, 1955; Pullam *et al.*, 1980). Here, I examined whether the addition of 0.2% Tween 80 can allow *S. intermedius* B196 to grow reproducibly under aerobic conditions without CO_2.

3.1.1. Tween 80 increases chain length of *S. intermedius* B196 under aerobic conditions.

In order to examine the effects of Tween 80 on the survival of B196 under conditions without CO_2, overnight cultures of B196 were grown in THY under anaerobic (5% CO_2, 5% H_2, 90% N_2), 5% CO_2, or aerobic conditions, in the presence or absence of 0.2% Tween. These cultures were then stained with the LIVE/DEAD BacLight Bacterial Viability Kit (Thermo Fisher Scientific), a combination stain of SYTO 9 and propidium iodide, and visualized under a fluorescence microscope.

The addition of 0.2% Tween 80 increased chain length in B196 grown under aerobic conditions, but not under conditions containing 5% CO_2 (Figure 3.1,

results not quantified). Under aerobic conditions without CO_2, B196 appears to form diplococci and stain green with SYTO 9, indicating cell membrane integrity; however, under conditions with 5% CO_2 or 0.2% Tween 80, B196 appears to have increased red propidium iodide staining compared to aerobic growth.. Increased dead cells may indicate autolysis during stationary phase, and thus viability of the cells during stationary phase should be properly tested.

The longer chain length in B196 cells grown in 5% CO_2 or with Tween 80 suggests that the cells were able to undergo more cell divisions, but differences in chain length may also indicate differing growth phases, or differences in environmental conditions (Evans *et al.*, 2014). Chain length may also play a role in increasing the final density of the cells; however, as optical density is not the best indicator of cell growth, other factors such as measuring nucleic acid content or metabolic activity may be done to verify these results. Additionally, the cells grown aerobically with 0.2% Tween 80 resembled the cells grown in 5% CO_2 and anaerobically, which supports the conclusion of Deibel & Niven (1955) that Tween 80 can replace the CO_2 in the growth of B196.

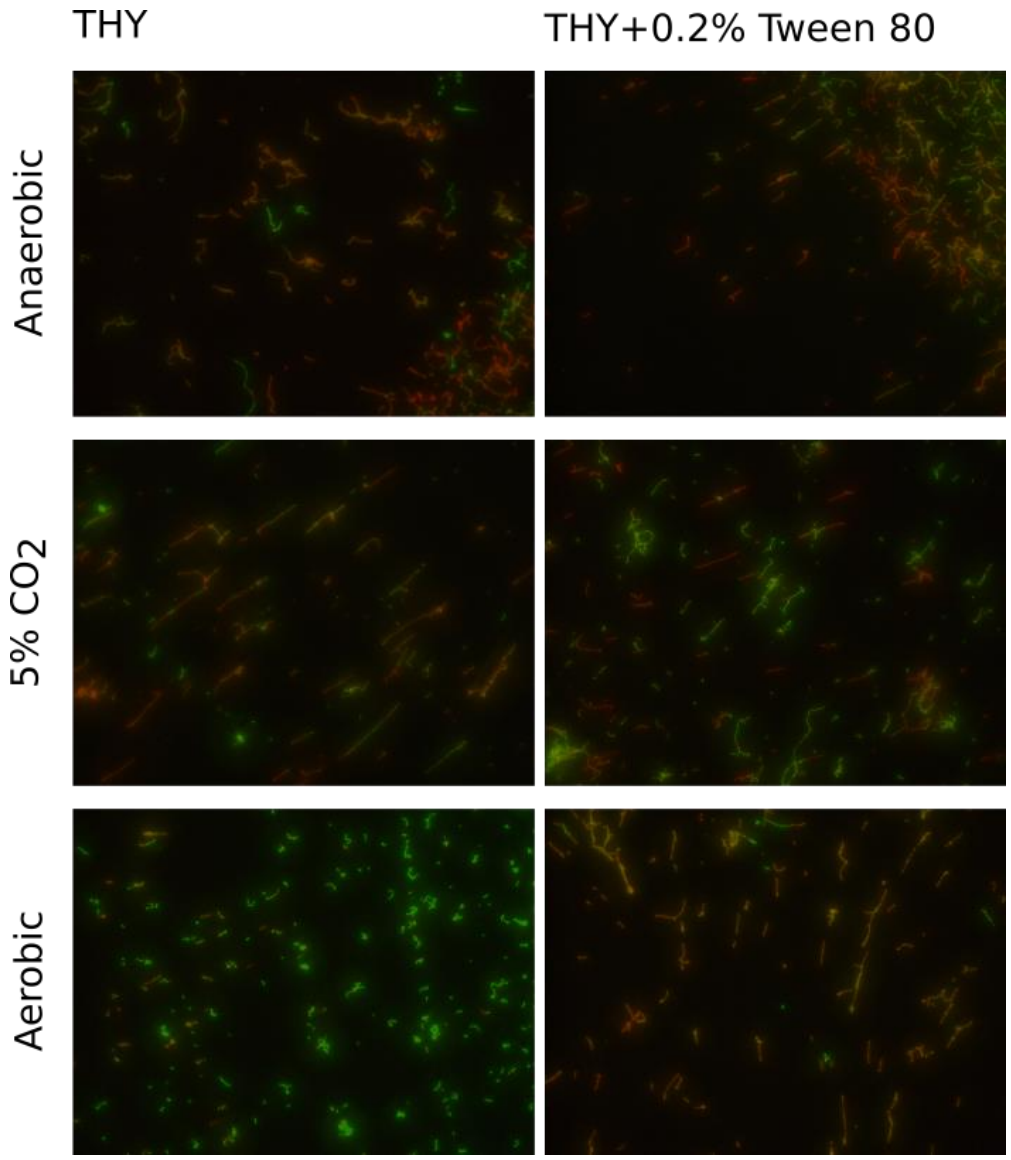

Figure 3.1: 0.2% Tween 80 rescues aerobic *S. intermedius* B196 growth. 1 µL of overnight B196 grown in THY at 37°C in 5% was added to 1 mL THY or THY + 0.2% filter-sterilized Tween 80 and incubated aerobically, anaerobically or in 5% CO_2 overnight. Cells were then stained using the Thermo Fisher LIVE/DEAD BacLight bacterial viability kit. Cells were then pelleted, washed and resuspended in 0.85% saline solution. Cells were diluted 1/10 in 0.85% saline solution, and 5 µL of cells were incubated onto a polylysine-coated coverslip for 20 minutes prior to visualization under a fluorescence microscope.

3.1.2. Tween 80 supplementation increases the aerobic growth reproducibility of *S. intermedius* B196 in a 96-well plate format.

In order to monitor the expression of the *lux* reporters over a prolonged period of time, I tested the effect of Tween 80 on B196 growth under aerobic conditions without CO_2 in a 96-well plate reader. The addition of 0.2% Tween 80 resulted in increased ($p = 9.0\times10^{-4}$) and less variable ($p = 5.1\times10^{-35}$) OD_{600} readings of *S. intermedius* B196 in a 96-well plate under aerobic conditions at 24 hours, reaching an average OD_{600} of 0.878 with a standard deviation of 0.045 (Figure 3.3), compared to growth without 0.2% Tween 80, which reached an average OD_{600} of 0.391 with a standard deviation of 0.369 (Figure 3.2); however, it appears that the growth of B196 results in the production of gas. These gas bubbles, trapped under the mineral oil layer, interfere with the OD_{600} readings of the plate reader, making it difficult to synchronize the growth curves of the various wells with the mineral oil overlay, as well as making the readings unreliable for expression dynamic calculations. Additionally, at the end of the 24h growth period, small colonies were observed forming at the bottom of the wells (not shown), which may have made readings inaccurate, as the cells were not uniformly distributed within the well.

3.2. *silAB*, *silCR*, and *silED* are all necessary for *S. intermedius* B196 SilCR-mediated inhibition of *S. constellatus* M505.

Initially, I wished to create a FRT-flanked spectinomycin cassette such that, after knocking out the genes, I could induce the expression of flippase to remove the spectinomycin resistance cassette, resulting in selection-free knockouts.

I was able to create Δ*silAB* and Δ*silE* through double homologous recombination. I was able to verify these knockouts through PCR, amplifying from a gene outside of the *sil* system, and was able to obtain product of the correct size for the two knockouts.

I made one attempt to express FLP recombinase in the B196 *sil* gene deletions and was unable to obtain any selection-free knockouts. Due to limitations in time, I decided not to pursue the construction of selection-free knockouts, and continued experiments with knockouts containing the spectinomycin resistance cassette.

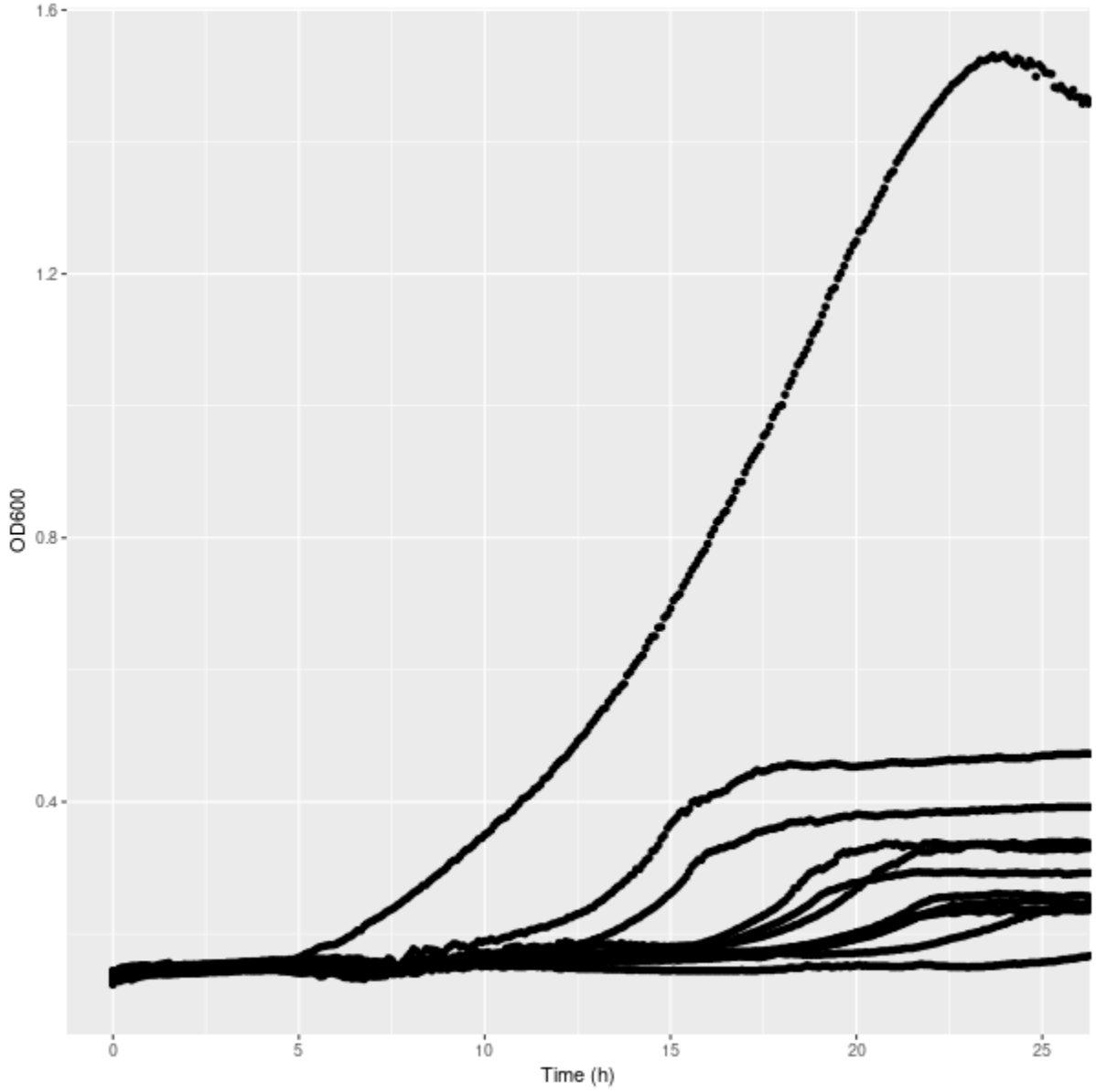

Figure 3.2: *Streptococcus intermedius* B196 does not reproducibly grow in an aerobic plate reader. Overnight cultures of B196 were grown in THY at 37°C in 5% CO_2. 15 µL of overnight culture was added to 135 µL THY, and grown at 37°C in a BioTek Synergy H1 Hybrid Multi-Mode Reader. Measurements were taken and cultures were shaken double-orbitally at 180 rpm every 5 min. After 24 hours, the average OD_{600} reached 0.391 with a standard deviation of 0.369

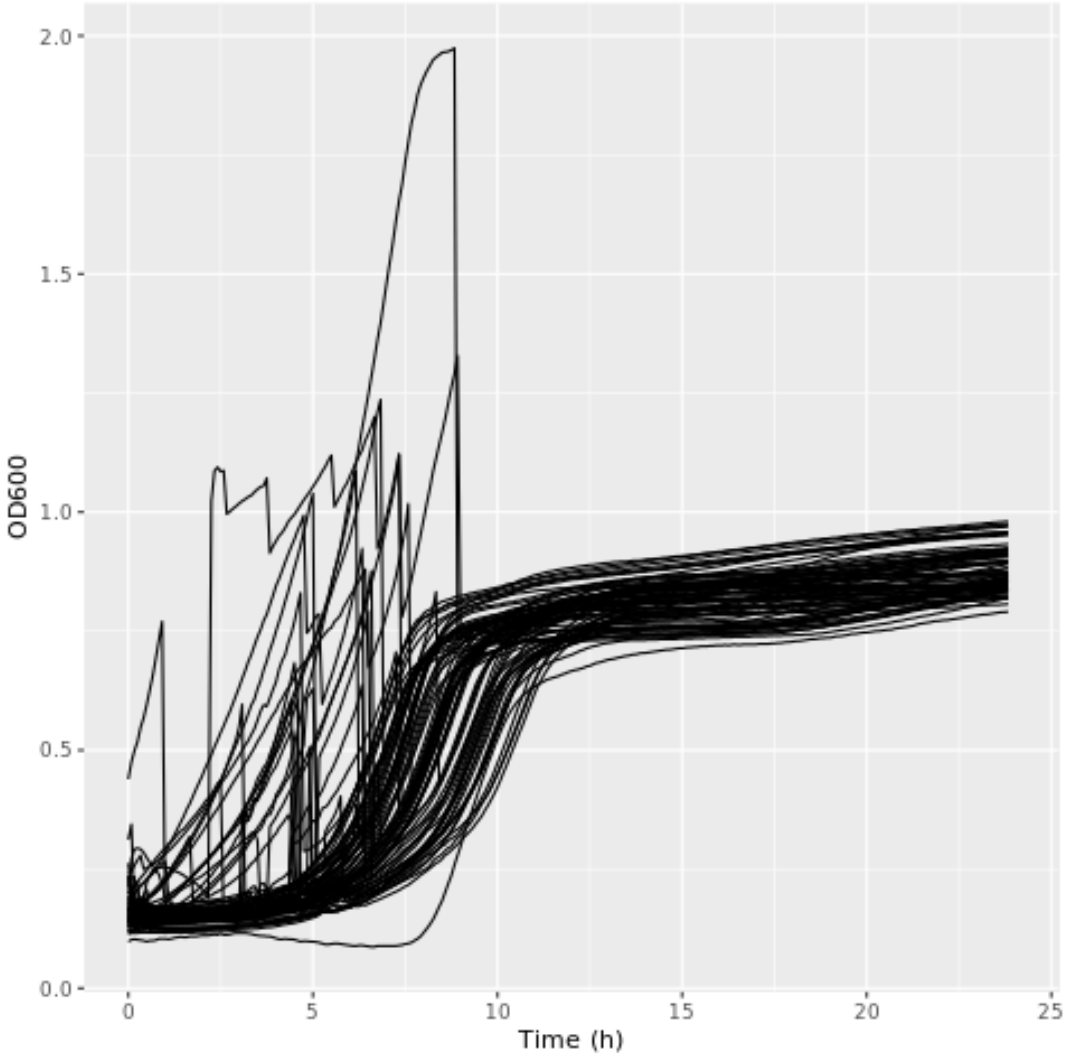

Figure 3.3: 0.2% Tween 80 is sufficient to reproducibly grow *S. intermedius* B196 in an aerobic plate reader, but raises measurement issues. 15 µL of overnight culture was added to 135 µL THY + 0.2% Tween 80, and grown at 37°C in a plate reader. Measurements were taken every 5 minutes and cultures were shaken double-orbitally at 180 rpm. Peaking growth and sudden falls were attributed to the formation of gas bubbles and subsequent popping, resulting in artefacts in the OD_{600} readings. After 24 hours, the average OD_{600} reached 0.878 with a standard deviation of 0.045.

3.2.1. *Streptococcus intermedius* B196 *sil* system knockouts show no inhibition against *S. constellatus* M505.

Mendonca *et al.* (2016) demonstrated that B196 inhibits the growth of *S. constellatus* M505 in a SilCR-dependent manner. I sought to reproduce this result, as well as test Δ*silAB* and Δ*silED* to see whether the other genes in the *sil* locus are required to inhibit the growth of *S. constellatus* M505. I was able to reproduce the result by Mendonca *et al*., showing that the B196 *silCR* knockout lost the ability to inhibit M505. I was also able to demonstrate that *ΔsilAB* and *ΔsilED* both lost the ability to inhibit the growth of M505 (Figure 3.4), indicating that *silAB*, *silCR* and *silED* are all required for B196 to inhibit the growth of M505.

3.2.2. Synthetic SilCR peptide rescues *S. intermedius* B196Δ*silCR*, but no other knockouts.

In this experiment, I looked at whether the addition of synthetic SilCR peptide can rescue the ability of B196Δ*silAB*, Δ*silCR* and Δ*silED* to inhibit the growth of M505. The addition of synthetic SilCR peptide rescued the zone of inhibition in the *silCR* knockout, reproducing the result in Mendonca *et al.* (2016); however, I was unable to rescue the zone of inhibition of Δ*silAB* or Δ*silED* (Figure 3.4), suggesting that both *silAB* and *silED* are required for the inhibition of M505 growth, and that their loss cannot be rescued by the addition of exogenous SilCR.

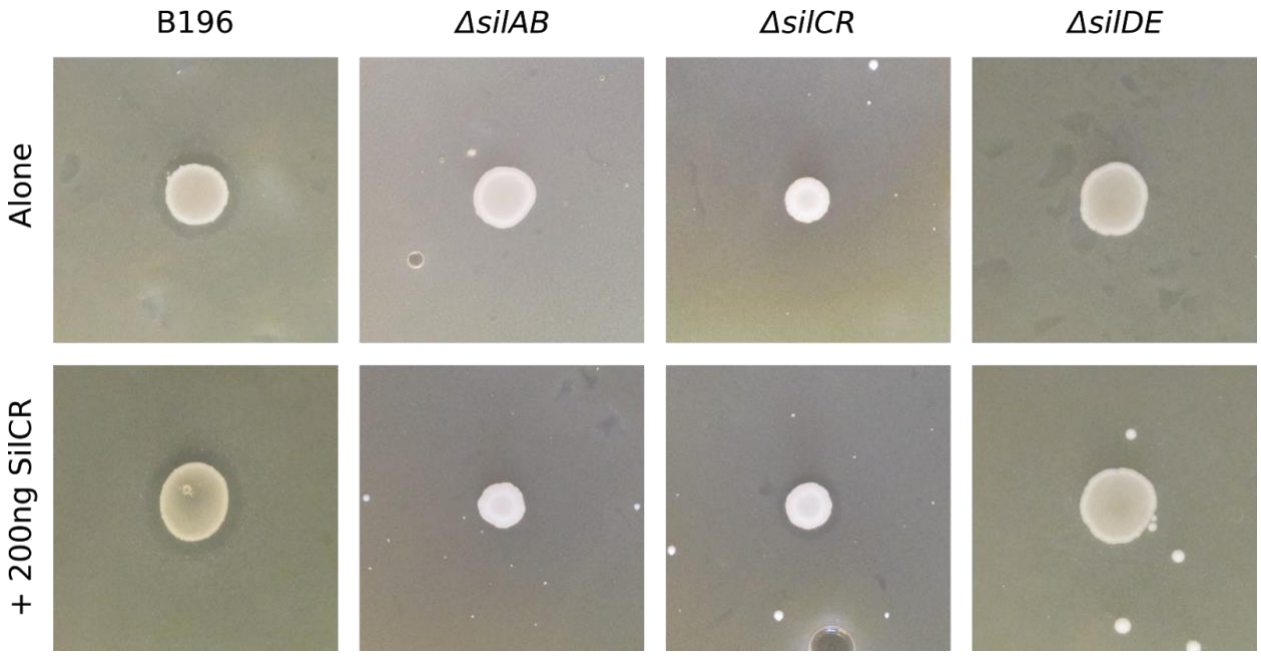

Figure 3.4: *silAB*, *silCR*, and *silED* are necessary for *S. intermedius* B196 inhibition of *S. constellatus* M505. 5 µL of overnight B196 *sil* system knockout cultures were spotted onto THY agar and incubated at 37°C in 5% CO_2 for 48 hours. 1 µL of 200 µg/mL SilCR peptide was spotted directly onto some colonies, and allowed to dry. 100 µL of overnight M505 culture grown anaerobically in THY at 37°C was added to 5 mL molten 1.5% THY agar, mixed, and poured over the THY agar. Plates were incubated overnight at 37°C in 5% CO_2. A zone of inhibition can be observed around B196. All *sil* system knockouts show no zone of inhibition. The zone of inhibition around B196Δ*silCR* can be rescued by the addition of 200 ng synthetic SilCR peptide, but none of the other knockouts were able to be rescued.

3.3. *sil system* transcription in *S. intermedius B196*

3.3.1. Variability in growth and viability affects reproducibility of *S. intermedius* B196 gene expression experiments

Using *luxABCDE* reporter constructs, I was able to measure the promoter activity of *silA*, *silCR* and *silE* over time. Repeating the experiments over three days, I found difficulties in synchronizing the growth curves, with the three experiments reaching a maximal rate of growth at 10.31, 11.86 and 7.81 hours, with a standard deviation of 0.21, 1.96, and 0.32 hours respectively (Figure 3.5, A-C), This may suggest that varying numbers of viable bacteria are being inoculated into each culture. These experiments also showed variability in maximal promoter activity in *silA* (21% relative standard deviation), *silCR* (71%) and *silE* (53%) (Figure 3.5, D-F). Using optical density as a proxy for growth, plotting normalized luminescence against optical density (Figure 3.5, J-L) showed varying transcription of the *sil* system genes relative to optical density, and the results show similar patterns when plotting normalized luminescence against time synchronized to maximal transcription (Figure 3.5, M-O).

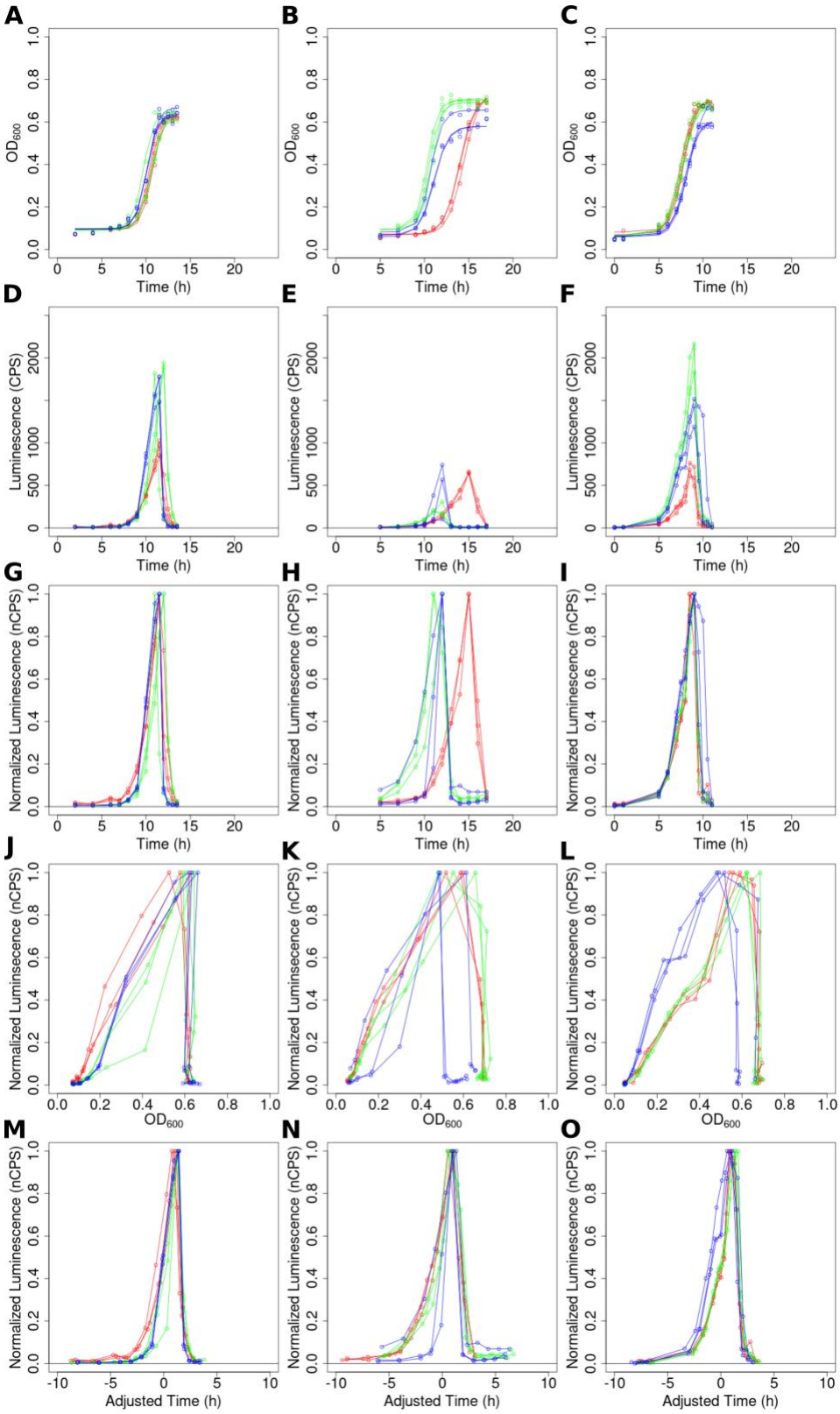
A
B
C
D
E
F
G
H
I
J
K
L
M
N
O
OD600
Time (h)
Luminescence (CPS)
Normalized Luminescence (nCPS)
Normalized Luminsecence (nCPS)
Adjusted Time (h)

Figure 3.5: Growth of *S. intermedius* B196 and expression of *sil* system genes over time across multiple experiments. Graphs show B196 transfected with reporter plasmids for the promoters upstream of *silA* (red), *silCR* (green), and *silE* (blue). Each column represents a single experiment. For each reporter strain, three cultures of THY + 100 µg/mL were inoculated from the same 0.4 OD_{600} culture of B196 reporter strain, and grown in 5% CO_2 at 37°C. 200 µL was removed every 0.5-2 hours for sampling. The amount of time for B196 to reach stationary phase varies between experiments (A–C). Additionally, maximal activity of the *sil* system promoters also varies between experiments (D–F). Plotting normalized luminescence against hours before or after the maximal growth rate (M-O) shows similar patterns to plotting normalized luminescence against optical density (J-L).

These results make it difficult to compare experiments across days. Three experiments performed in parallel with colonies selected from the same plate (Figure 3.6) still show difficulties in synchronizing the growth curves, reaching maximal growth at 15.68 hours with a standard deviation of 1.12 hours (Figure 3.6, A-C), but showed significantly lower variability in maximal promoter activity in *silCR* (6.9% relative standard deviation, $p = 2.3\times10^{-3}$) and *silE* (7.0%, $p = 6.1\times10^{-3}$), but not in *silA* (9.9%, p = 0.12) (Figure 3.6, D-F). Maximal *silA* promoter activity was also 331 CPS lower than the experiments done across multiple days (p = 0.042), but the maximal activity of the *silCR* and *silE* promoters were not significantly different (p = 0.352, 0.344). Normalized luminescence plotted against optical density also showed lower levels of variability (Figure 3.6, J-L).

3.3.2. *silA* transcription precedes *silE* transcription.

As the growth curves were not synchronized, I could not use time to calculate the promoter activity order of the *sil* system genes. Instead of time I decided to use OD_{600} as a proxy for growth, and calculated the OD_{600} at 10% maximal promoter activity. I linearly interpolated the two closest data points to 10% maximal promoter activity to find the OD_{600} at the time of measurement. Linear interpolation only holds if the relationship between the two time points are linear, which may not be true. A greater sampling frequency could be used to

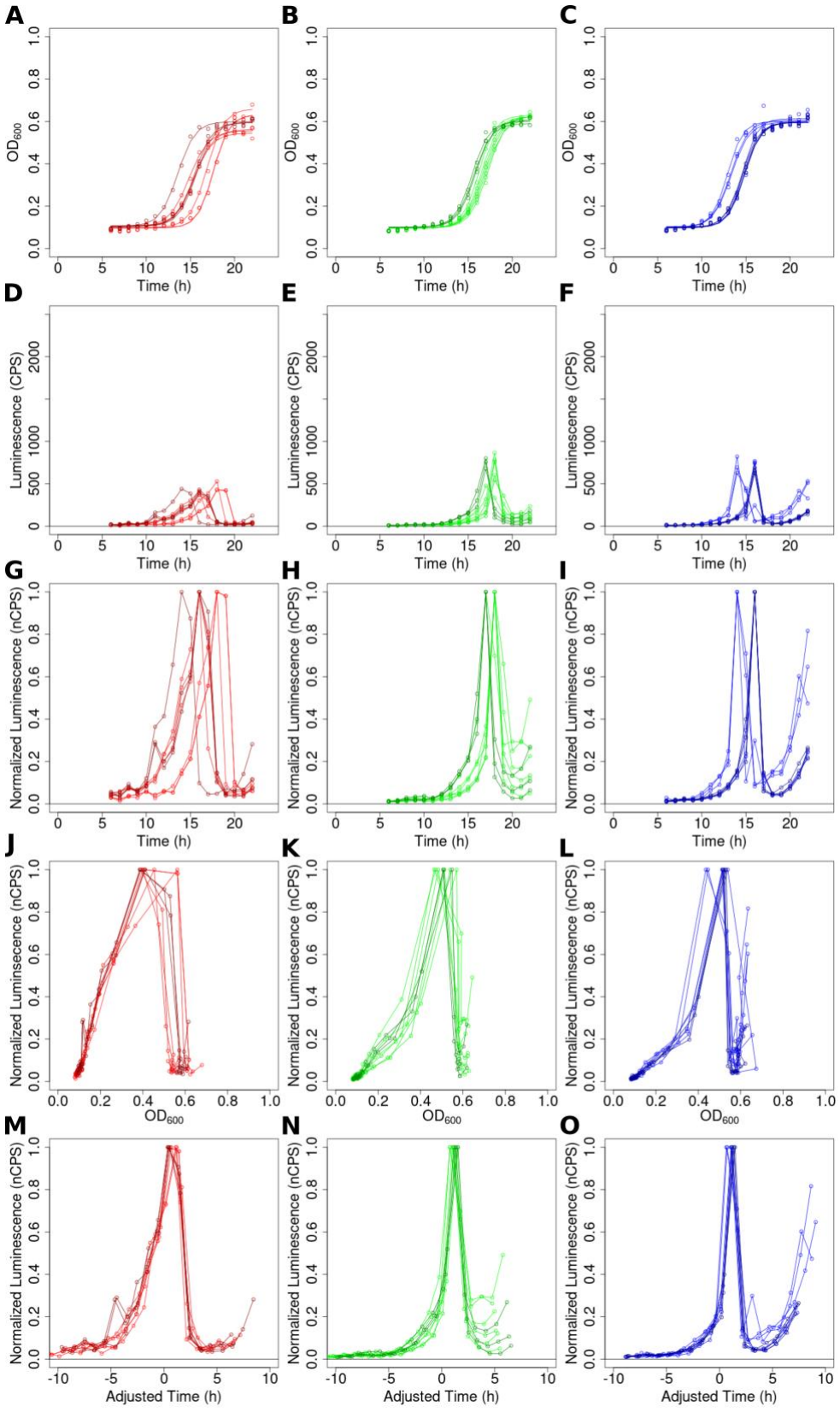
A
B
C
D
E
F
G
H
I
J
K
L
M
N
O
OD600
Time (h)
Luminescence (CPS)
Normalized Luminescence (nCPS)
Adjusted Time (h)

Figure 3.6: Growth of *S. intermedius* B196 and expression of *sil* system genes over time between colonies from the same plate. Graphs show B196 transfected with reporter plasmids for the promoters upstream of *silA* (red), *silCR* (green), and *silE* (blue). Each individual colony is represented by a different shade. For each reporter strain, three cultures of THY + 100 µg/mL were inoculated from the same overnight culture of B196 (n=3), and grown in 5% CO_2 at 37°C. 200 µL was removed every 0.5-2 hours for sampling. Despite variance in growth synchronicity (A-C) and promoter activity timing (D-I), the data shows reproducible normalized luminescence against optical density (J-L). Synchronizing normalized luminescence to the point of maximal growth (M-O) also shows reproducible promoter activity over time.

reduce the error introduced by a non-linear relationship. Additionally, after synchronizing the promoter activity data to the point of maximal growth, I linearly interpolated the time from the two closest data points to the 10% maximal promoter activity so that I could compare the time before maximal growth at which promoter activity reached 10% maximal.

In the data pooled together from the three experiments done over multiple days, *silA*, *silCR*, and *silE* promoter activity reached 10% maximal at OD_{600} 0.118, 0.155 and 0.148 and a standard deviation of 0.021, 0.052 and 0.052 respectively. Interpolated time puts the 10% maximal promoter activity at 2.61, 2.25 and 1.95 hours before the time point of maximal growth, with a standard deviation of 0.71, 1.25 and 0.84 respectively. Due to the high variance in the data, there was no significant difference in the OD_{600} or time before maximal growth at 10% maximal activity ($p = 0.57, 0.71$).

In the data collected from three colonies on a single plate, *silA*, *silCR*, and *silE* promoter activity reached 10% maximal at OD_{600} 0.117, 0.178 and 0.195 and a standard deviation of 0.004, 0.034 and 0.004 respectively. Interpolated time puts the 10% maximal promoter activity at 4.55, 2.01 and 1.49 hours before the time point of maximal growth, with a standard deviation of 0.60, 0.62 and 0.10 respectively. The promoter activity of *silA* reached 10% maximal activity at an OD_{600} 0.07 less than *silE* ($p = 0.003$), and 3.07 hours earlier ($p = 0.017$, not significant after multiple test corrections). Compared to *silA*, the *silCR* promoter

did not reach 10% maximal activity at a significantly different OD_{600} ($p = 0.112$) or time ($p = 0.059$). *silCR* and *silE* promoters showed no significant difference in the OD_{600} ($p = 0.456$) or time ($p = 0.264$) at 10% maximal activity.

3.3.3. *sil* system knockouts lowers the transcription of all other *sil* system genes.

As I was unable to measure promoter activity in the B196 gene deletion strains due to a shared spectinomycin resistance cassette between the knockout and the *lux* reporter plasmids, I sought out alternate means to quantify *sil* system transcription to determine how the knockouts affected the transcription of the *sil* system. I decided to use real-time quantitative PCR (RT-PCR) to measure the transcription levels of the various *sil* system genes. I chose to sample cultures at an OD_{600} of 0.3, which corresponded with approximately 30% of maximal promoter activity of *silCR*.

RNA extractions on B196 proved difficult, and only low levels of RNA were able to be obtained. Being unable to normalize the amount of RNA loaded into each well, I decided to normalize transcription levels to that of a housekeeping gene such that I could compare transcription levels between wells. Housekeeping genes function as an internal reaction control that are chosen to have as little variance in transcription, and not change transcription rate in response to experimental factors (Kozera & Rapacz, 2013).

I initially considered using *sodA*, a superoxide dismutase, as the reference gene for transcription, as it is a known housekeeping gene (Wen *et al.*, 2016) and I already had primers designed for *sodA*; however, further research indicated that *sodA* has variable transcription compared to other housekeeping genes (Wen *et al.*, 2016). From the list in Wen *et al*. (2016), I chose *rpoB* as the housekeeping gene*,* which codes for the β subunit of RNA polymerase, as it is present as a single copy in the B196 genome, and in Wen *et al.* (2016) appears to have the most stable transcription during the exponential phase. In the future, housekeeping genes that have been validated in *Streptococcus*, such as *gyrA* and *proS* (Graham *et al.*, 2003) would provide better validity as housekeeping genes for transcription, and multiple housekeeping genes can be used at once to increase resolution and accuracy (Kozera & Rapacz, 2013).

All of the no reverse transcriptase controls were >5 Cq above the target sequences, indicating that the controls had at most 32-fold less DNA template compared to RNA template in the samples. No template controls showed no signal, indicating that no primer dimers were formed.

RT-PCR results show that each of the strains Δ*silAB*, Δ*silCR*, and Δ*silED* lower the transcription of the other two *sil* system genes that were not knocked out (Figure 3.7). Compared to the wild type, *silA* transcription was lowered by 85% in Δ*silCR* and 70% in Δ*silED. silCR* transcription was reduced by 97% in Δ*silAB* and 95% in Δ*silED. silE* transcription was lowered by 98% in Δ*silAB* and

99% in Δ*silCR* when compared to the wild type. Given that the loss of any one of the operons results in a lowered transcription of each of the other two operons, it is likely that all three operons are required as part of the regulatory network.

3.3.4. Addition of synthetic SilCR to Δ*silAB*, Δ*silCR*, and Δ*silED* partially rescues *sil* system transcription.

Induction with exogenous SilCR resulted in a 12.77-fold increase in transcription of *silA*, and a 4.56-fold increase in *silE* transcription in Δ*silCR*. Addition of exogenous SilCR to Δ*silED* resulted in a 9.22-fold increase in *silA* transcription, and a 4.56-fold increase in *silCR* transcription. Incubation of Δ*silAB* with synthetic SilCR peptide increased *silCR* transcription by 1.2-fold, and increased *silE* transcription 1.08-fold. Addition of exogenous SilCR to the wild-type B196 strain increased the transcription of *silA*, *silCR*, and *silE* by 1.19-, 1.29-, and 1.44-fold, respectively (Figure 3.7).

These results suggest that *silA* is necessary to drive the transcription of *silCR* and *silE*, even in the presence of exogenous SilCR. The data also suggests that exogenous SilCR is capable of driving the transcription of *silA* and *silE* in Δ*silCR*, and is also capable of fully restoring the transcription of *silA*, but only partially restoring the transcription of *silCR*, in Δ*silED*. As only one experimental run was completed, further experiments should be performed to confirm these results.

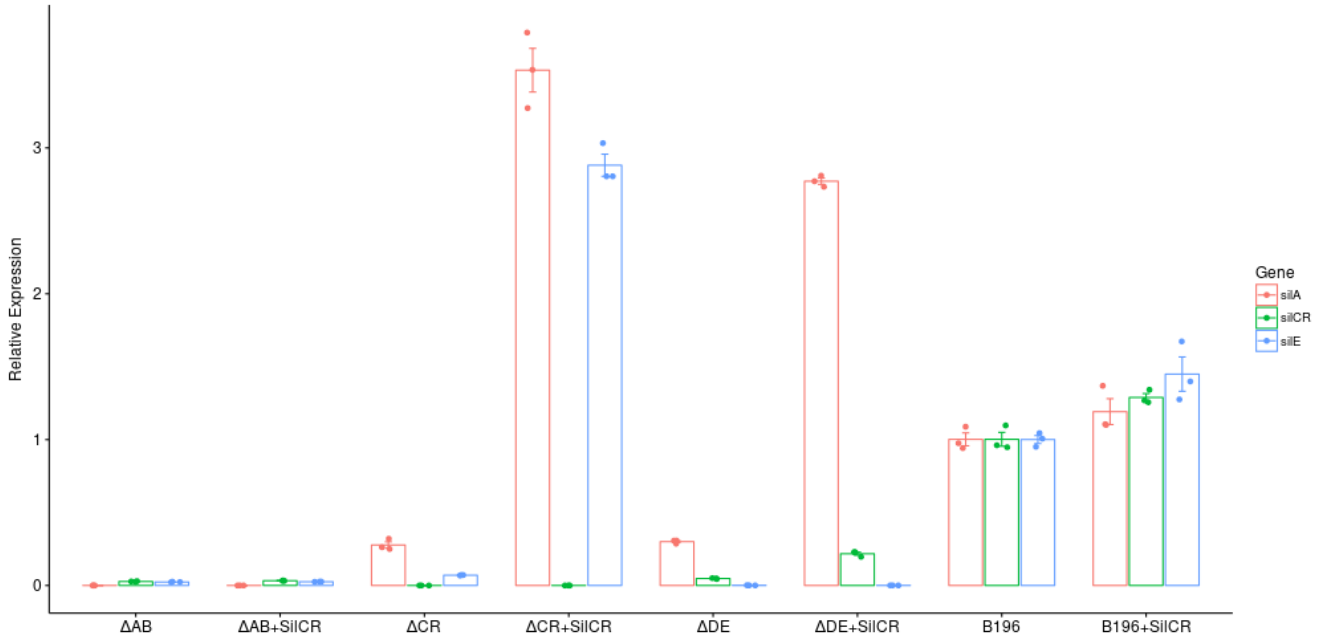

Figure 3.7: Transcription of the *Streptococcus* invasion locus genes in various *S. intermedius* B196 *sil* locus knockouts. B196 *sil* system knockouts were grown in THY + 100 µg/mL spectinomycin to an OD_{600} of 0.3. Synthetic SilCR peptide was added to some cultures to a total concentration of 50 nM, and all cultures were incubated at 37°C in 5% CO_2 for 30 minutes. 3 mL of cells were pelleted. RNA extraction was carried out with TRIzol reagent (Invitrogen) followed by column purification using the Qiagen RNAeasy Kit with on-column DNase digestion. cDNA was generated from 10 µL of RNA with Superscript III First-Strand Synthesis System (Invitrogen) using random hexamer primers. Real-time PCR primers can be found in Table 2. Real-time PCR reactions were performed in a CFX96 Real-time PCR machine (BioRad) at 55°C. 20 µL reactions were performed in triplicate with 10 µL Sso Fast Evagreen supermix (BioRad), 1 µL cDNA and 500 nm of primer. The specificity of the product was determined by melt curve analysis. No-template controls and RT-free RNA controls were >5 Cq above the target sequences. Gene transcription was normalized to *rpoB* as a control.

3.4. Predicted promoters and terminators in the *sil* locus provide suggestions into operon structure.

3.4.1. BPROM predicts σ^{70} promoters upstream of *sil* system genes.

Using BPROM (Solovyev & Salamov, 2011), I scanned regions upstream and downstream of *sil* system genes for σ^{70} promoters. I was able to predict promoters upstream of *silA*, *silCR* and *silE*, as well as on the reverse strand downstream of the *silCR* gene, similar to the relative position of *silC* in the *sil* system in Group A *Streptococcus* (Figure 1.3, Hidalgo-Grass *et al.*, 2002).

The accuracy of the predictions may be questioned, as BPROM is designed to search for *E. coli* promoters, and was not specifically designed for searching for promoters in *Streptococcus*. Additionally, the BPROM prediction model is mainly based on σ^{70} promoters (Solovyev & Salamov, 2011), and may miss promoters which bind to alternate sigma factors (Opdyke *et al.*, 2003).

BPROM predicts promoters by searching for five motifs from +10 to -60 of the transcription start site. The two most conserved motifs are the -10 and -35 sequence elements, which are found in promoters regulated by σ^{70} transcription factor. Both elements are AT-rich to aid in DNA unwinding; -10 sequence element has a consensus sequence of TATAAT, and the -35 sequence element has a consensus sequence of TTGAACA (Hook-Barnard & Hinton, 2007).

The genus *Streptococcus* is a low GC content taxon (Gao *et al.*, 2014), ranging in GC content from 33.79% to 43.40%, with *S. intermedius* B196 has a

GC content of 37.6%. Due to the high AT content in the B196 genome, it is possible that BPROM overpredicts the number of promoters, as the model it uses for promoter prediction searches for the -10 and -35 sequence elements, which is more likely to result in false positives in AT-rich regions (Stoll *et al*., 2009).

3.4.2. Fourteen Rho-independent terminators are predicted in the *sil* locus and accessory region of *S. intermedius* B196.

Rho-independent terminators, or intrinsic terminators, consist of an 7-10bp GC-rich inverted palindrome followed by a poly-T in DNA. When transcribed, the poly-U tract in RNA stalls the progress of RNA polymerase, allowing the palindromic sequences to form a hairpin loop at the exit channel of RNA polymerase, which weakens the RNA–DNA hybrid and initiates the events that result in termination (Ray-Soni *et al*., 2016).

Submitting the B196 *sil* locus and accessory region into ARNold (Naville *et al.*, 2011), I predicted 14 terminators, 8 of which are forward-reverse strand terminator pairs (Figure 3.8). Terminators were predicted downstream of the *silAB* operon and *silCR* operon, but not after the *silED* operon, suggesting read-through transcription from *silED* to *silCR* may occur.

ARNold uses models trained on *Bacillus subtilis* and *E. coli* in order to predict the terminators (Naville *et al.*, 2011), and thus may not be optimized for predicting terminators in *Streptococcus*.

It is possible that Rho-dependent terminators exist within the *sil* system, and would not have been detected by ARNold; however, no significant homolog to the Rho protein were found in either *Streptococcus pneumoniae or S. pyogenes* (Washburn *et al.*, 2001). A search with Protein BLAST (Boratyn *et al.*, 2013) found no significant homologs to the *E. coli* Rho protein in the SAG, which suggests that no Rho-dependent terminators should exist in the *sil* locus.

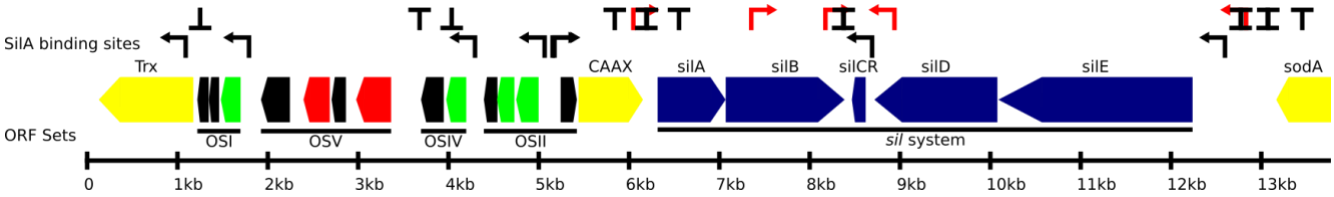

Figure 3.8: Predicted σ^{70} promoters, rho-dependent terminators, and SilA-binding sites in the *S. intermedius* B196 *sil* system and accessory region. σ^{70} promoters (red arrows) were predicted using BPROM (Solovyev & Salamov, 2011). Rho-independent terminators (T, ⊥ for reverse-strand terminators) were predicted using ARNold (Naville *et al.*, 2011). SilA-binding sites (black arrows) were predicted by Mendonca *et al.* (2016). Figure adapted from Mendonca *et al.* (2016).

Chapter 4: Discussion and Conclusion

This study aimed to provide new information about the *sil* system in the *Streptococcus* Anginosus Group, a group of microbial organisms that inhabit the upper respiratory, gastrointestinal, and urogenital tracts, but have also been associated with disease. The *sil* system is a two-component quorum-sensing system initially identified in Group A *Streptococcus,* but similar systems have been identified in Group G *Streptococcus*, and most recently in the SAG. The regulation of the *sil* system in the SAG has not been examined, and in this study I aimed to examine the transcriptional dynamics of the *sil* system in *S. intermedius* B196. Furthermore, based off the functioning of the *sil* system in GAS, as well as the predicted SilA-binding sites, I wished to build a model on how the individual genes in the B196 *sil* system regulate each other.

To study the *sil* system, I generated knockouts of *silAB* and *silED* in *S. intermedius* B196. In combination with the *silCR* knockout from Mendonca *et al.* (2016), all three predicted operons of the B196 *sil* locus have been knocked out. By examining the gene transcription of the *sil* system genes in wild-type B196 and these knockouts, as well as in the presence of exogenous SilCR peptide, new knowledge was obtained about the functioning of the *sil* system in *S. intermedius* B196.

4.1. The effect of Tween 80 on the growth of *S. intermedius* B196.

It has been previously found that Tween 80 can substitute for CO_2 for the growth of streptococcal species (Deibel & Niven, 1955; Pullam et al., 1980) in liquid culture, although it appears to inhibit growth and hemolysis in blood agar plates. I confirmed the findings that Tween 80 aids the growth of *S. intermedius* B196 in the absence of CO_2; however, staining indicates that Tween 80, and normal growth in the presence of CO_2 seems to result in the disruption of the cell membrane of B196.

The presence of propidium iodide staining indicates impaired cell membrane integrity. Both the propidium ion of propidium iodide and SYTO 9 bind to double-stranded DNA in a sequence-independent manner, and both result in greater fluorescence (red for propidium iodide, green for SYTO 9) when bound to DNA compared to their unbound state. SYTO 9 can pass through the cell membrane, and stains all cells; however, the propidium ion is doubly charged and cannot pass through intact cell membranes, and thus supposedly stains only dead cells. As the propidium iodide binds more tightly with DNA than SYTO 9 stain, propidium iodide should displace the SYTO 9 stain (Stocks, 2003).

It is known that some species of *Streptococcus* autolyse during stationary phase. It is thought that autolysis allows for the release of DNA into the environment, which can then be taken up by other competent cells (Steinmoen *et al.*, 2002). Competence in *Streptococcus* is triggered by the two-component

system ComDE sensing the competence stimulating peptide, which is produced and secreted by the cell, and induced competence has been found to trigger to autolysis in a subfaction of the cell population (Steinmoen *et al.*, 2002). It is possible that, under conditions containing CO_2 or Tween 80, B196 can reach stationary phase sooner and undergo autolysis, thus explaining the cells stained red that we observed. If the cells are undergoing autolysis, I would expect cell viability to decrease during stationary phase. As only cells from the 24 hour time point were examined, it is not possible to know if the cell viability differences reflect differences in growth stage. Further research should be done into observing when during growth propidium iodide staining first occurs.

It is possible that the cells grown aerobically without Tween 80 or CO_2 were unable to reach the stationary phase of growth, given the lower cell density and shorter chain length, and may have been unable to reach the growth state required for autolysis. It is possible that autolysis in B196 is driven by competence, as competence in *Streptococcus* is also tightly regulated to specific growth phases (Steinmoen *et al.*, 2002). This can be tested by adding exogenous competence stimulating peptide to these aerobic cultures and observing whether this is sufficient induce autolysis.

Propidium iodide staining can also indicate cell division (Shi *et al.*, 2007), as the cell membrane is partially disrupted during the process of binary fission; however, it is unlikely in this case as the staining time is much lower than the

doubling time of the organism, and other growth experiments have shown that B196 should be in stationary phase after 24 hours of growth.

An alternate explanation is that Tween 80 disrupts the cell membrane by acting as a surfactant (Nielsen *et al.*, 2016), lowering the surface tension between the cell membrane and the media. While Tween 80 may not cause cell lysis at low concentrations, it is possible that the disrupted cell wall is permeable enough that propidium iodide is able to enter the cell and stain DNA; however, this does not explain the increased propidium iodide staining in the cells grown in 5% CO_2 which were not exposed to Tween 80.

An alternate hypothesis is that the cells are reaching different stages of growth. SYTO 9 staining in the aerobic cultures of B196 without CO_2 without Tween 80 indicate that the cell membrane is still intact, which implies the cells are still alive; but as the chain length of the aerobic cultures are shorter than those grown in CO_2, this suggests that B196 does not reproduce in the absence of CO_2. Since the aerobic bacteria did not replicate in the absence of CO_2 or Tween 80, this suggests that the overnight cultures are at different growth phases. This may be responsible for the change in membrane permeability, as some streptococci are known to undergo autolysis at high population densities (Mellroth *et. al*, 2012); however, preliminary experiments could not confirm autolysis in B196 (data not shown).

A third hypothesis is that the cells grown with Tween 80 or in CO_2 have a higher membrane potential. The highly charged propidium ion has been shown to pass through the cell membrane of multiple anaerobically grown bacterial species due to the high membrane potential (Kirchhoff & Cypionka, 2017). It is possible that B196 also generates a high membrane potential during growth, which results in the permeability of the cell membrane for the propidium ion, allowing for living cells to be stained red during propidium iodide staining.

Additionally, addition of Tween 80 may disrupt gene expression in B196; although there is no evidence that Tween 80 does anything other than substitute for the presence of CO_2, it is possible that Tween 80 increases permeability of the cell membrane and thus possibly change the gene expression of the organism. Thus, for these reasons, I decided not to use Tween 80 in the growth of B196, and instead sampled cultures grown in 5% CO_2.

4.2. The role of *sil* locus genes on the inhibition of SAG member *S. constellatus* M505.

In both SAG and GAS, adjacent to the *sil* locus is an accessory region, containing genes resembling bacteriocins. In GAS, the associated region lies downstream of the *sil* locus; in SAG, the region lies upstream, and is composed of a variable cluster of different open reading frame sets. In *S. intermedius* B196, Mendonca *et al.* (2016) showed that inhibition of SAG member *S. constellatus*

M505, lacking the associated bacteriocin cluster, by B196 is *silCR* dependent, and addition of exogenous SilCR peptide rescues this loss of inhibition in Δ*silCR*, suggesting that genes encoding for a bacteriocin and its immunity protein lie in the associated bacteriocin cluster, whose expression is driven by the *sil* system.

The lack of inhibition in the *silAB* knockout in the presence of synthetic SilCR suggests that SilA is responsible for driving the expression of the bacteriocin(s) that inhibit M505 growth, and the presence of predicted SilA-binding sites upstream of genes in the associated bacteriocin cluster supports this hypothesis (Mendonca *et al.*, 2016).

The inability for the zone of inhibition in the *silED* knockout to be rescued by SilCR may suggest that SilDE is required for the export of the bacteriocin(s) that are responsible for inhibiting M505 growth. No studies have been done on bacteriocin export by SilDE; however, it is hypothesized that SilDE is capable of exporting bacteriocins, due to its similarity to the bacteriocin exporter BlpAB (Wang *et al.*, 2018).

4.3. Temporal expression of *sil* system genes.

Growth and promoter activity of B196 *sil* system genes appear to be highly variable and difficult to reproduce. Even while following the same protocol, there is variance in the amount of time it takes for the cells to reach stationary phase (Figure 3.5, A-C, Figure 3.6, A-C). As the data suggests that cell death may be

occurring during stationary phase (Figure 3.1), this variability in growth may be due to variable inoculation of viable cells. It may be possible to control for this by measuring cell viability over time, and only inoculating from cultures that are fully viable.

Variability in promoter activity appears sensitive to experimental conditions. Promoter activity relative to optical density and maximal promoter activity varies between experiments, but I was able to reduce variation by controlling for changes in experimental conditions by running experiments concurrently and by selecting colonies grown on the same plate. For the experiments done on multiple days, I used a bacterial stock that had undergone fewer freeze-thaw cycles, which may explain the greater *silA* maximal promoter activity in the experiments done over multiple days compared to the those done in parallel; however, there is still variability in maximal promoter activity across days.

I could not combine the data done in three independent experiments and the three parallel experiments due to slight changes in experimental protocol; in the three independent experiments, the cultures were inoculated with cultures grown to 0.4 OD_{600}, whereas the three parallel experiments were inoculated with cultures grown overnight diluted to 0.1 OD_{600}.

The data pooled from the three independent experiments are too variable to suggest any order of expression, and if further data is collected, it may be possible find a trend in the order of gene expression.

In the data from the three parallel experiments, *silA* promoter activity reaches 10% maximum earlier than *silE* when using OD_{600} as a proxy for growth. The initial expression of *silA* was expected, as I hypothesized that the SilA response regulator is responsible for activating the promoters of *silCR* and *silE* via the predicted SilA-binding sites; however, I was unable to show that *silA* promoter activity reached 10% maximal activation significantly earlier than *silCR*. Although there was not a significant difference in the order of promoter activation between *silA* and *silCR* or *silCR* and *silED*, across both experiments the *silA* promoter reached 10% maximal activation at the lowest OD_{600} and earliest time, followed by *silCR* and then *silE*. Further research should be done to determine whether this trend is significant over larger pools of data.

OD_{600} is not the best proxy for cell growth, as optical density measurements are susceptible to changes in cell size, filamentation and growth phase, and loses accuracy in cultures of high density (Stevenson *et al.*, 2016). Alternate measurements of growth, such as nucleic acid content or metabolic activity may be required to verify these results.

4.4. Interactions between the *sil* system genes

All three of Δ*silAB*, Δ*silCR* and Δ*silED* showed a reduction in transcription of the other two measured *sil* system genes when compared to the wild type. This suggests that each of the three genes play a role in upregulating the transcription

of the other two; however, the reduction in *silA* transcription in the knockouts is of specific interest, as there is no predicted SilA-binding site directly upstream of the *silA* gene (Mendonca *et al.*, 2016). In GAS, microarray analysis identified that *silB* was slightly upregulated upon addition of SilCR, but this was not detected in real-time RT-PCR (Belotserkovsky *et al.*, 2009).

Upstream of the *silA* gene lies *caax*, a gene coding for a putative CAAX protease with a predicted SilA-binding site in its promoter region; however, this SilA-binding site is inconsistent with other predicted SilA-binding sites, as the second direct repeat appears different (Mendonca *et al.*, 2016). This SilA-binding site may also upregulate the transcription of *silA*, explaining why transcription levels of *silA* are suppressed in the *sil* system gene knockouts; however, a predicted terminator lies between *caax* and *silA* (Figure 3.8), which may suggest that SilCR-dependent *silA* transcription may be driven by something other than SilA-binding.

Assuming that each of three knockouts completely disrupt the *sil* system, the data suggest that *silA* has the highest basal transcription, followed by *silE,* with basal *silCR* transcription being the lowest. High basal *silA* transcription was expected, as SilAB is responsible for both driving gene transcription and sensing SilCR in the extracellular environment. SilCR activity is hypothesized to be dependent on the presence of SilDE, so it can be argued that *silCR* should not be expressed without the presence of SilDE; however, one could equally argue that

the system should only express the ABC transporter in the presence of the signal peptide, unless SilDE plays a role in exporting other short peptides, such as bacteriocins.

As the data was collected at only one time point, it may not be representative of the basal transcription of the system throughout all stages of growth.

The inability for synthetic SilCR peptide to increase the transcription of either *silCR* or *silED* in the *silAB* knockout supports the hypothesis that SilA is the response regulator driving the system, as the downstream genes cannot be upregulated without the corresponding response regulator.

The stimulation of Δ*silCR* with the SilCR peptide restored *silA* and *silE* transcription past the unstimulated wild type, demonstrating that exogenous SilCR can rescue *silA* and *silE* transcription. This result corresponds with the result in Mendonca *et al.* (2016), with a few minor differences. Experiments by Mendonca *et al.* showed a 138-fold increase of *silED* transcription in Δ*silCR* in the presence of exogenous SilCR, compared to the 41-fold increase in transcription found in this experiment, and Mendonca *et al.* found a insignificant decrease in *silED* transcription in wild type in the presence of SilCR, compared to the 1.08-fold increase in this experiment. These differences may be explained due to differences in experimental conditions; Mendonca *et al.* performed the experiments on solid media compared to these experiments in liquid media, which

may affect SilCR availability or other expression patterns. Additionally, the cells in the colony on solid media are likely in different growth phases due to differences in nutrient availability, which may also result in differing gene expression.

In Δ*silED*, exogenous SilCR stimulated the transcription of *silA* to levels past that of the unstimulated wild type, reaching levels similar to that of the stimulated *silCR* knockout; however, despite being upregulated, *silCR* is unable to reach wild type transcription levels. In Group A *Streptococcus*, *silCR* is part of the same operon as *silED*, and a SilA-binding site was not predicted upstream of *silCR* (Belotserkovsky *et al.*, 2009); however, in the B196, a SilA-binding site lies upstream of *silCR* (Mendonca *et al.*, 2016). In B196, ARNold (Naville *et al.*, 2011) does not predict the presence of a Rho-independent terminator between *silED* and *silCR*, and BPROM (Solovyev & Salamov, 2011) predicts a promoter upstream of *silCR* between *silCR* and *silED*, indicating that *silCR* transcription may be driven by both the promoter upstream of *silCR* and the promoter upstream of *silED*. Although the upstream promoter of *silCR* appears to be active in the absence of the *silED* promoter (Figure 3.5, 3.6), the transcription of *silCR* in the exogenous SilCR experiments is relative to the wild type, which includes transcription by both the promoter directly upstream of *silCR* and possibly the promoter upstream of *silED.* Given that, relative to the wild type, *silCR* transcription is not fully rescued by the addition of exogenous SilCR peptide in the *silED* knockout, the data supports the hypothesis that transcription of *silCR* is initiated by both the *silCR*

promoter and the *silED* promoter. It may also be possible that the *silED* region contains an enhancer that is necessary to fully rescue SilCR-induced transcription.

Wild-type B196 increases transcription of all *sil* system genes upon stimulation with exogenous SilCR, but stimulated *silA* and *silE* transcription are much lower than the stimulated transcription in the *silCR* and *silED* knockouts. This suggests that there may be a negative feedback loop built into the system that may be disrupted in the *silCR* and *silED* knockouts.

In Group A *Streptococcus*, the *sil* system contains a *silC* gene which overlaps *silCR* on the opposite strand by 70%, which may result in competitive transcription (Eran *et al.*, 2007). It is possible a similar system exists in the SAG *sil* system; a promoter search with BPROM (Solovyev & Salamov, 2011) found a predicted promoter on the reverse strand of *silCR* (Figure 3.8), but no attempt has been made to find the *silC* transcript.

4.5. Future Directions: towards a model in the expression of the *sil* system in *S. intermedius* B196.

My data has provided new information into the dynamics of the *sil* system in *S. intermedius* B196. These results suggest that *silA* drives the transcription of *silCR* and *silED*, and that *silA* transcription is upregulated in the presence of exogenous SilCR, though the mechanism for the *silA* upregulation is unknown.

Evidence from this study also suggests that an intact *sil* system prevents excess upregulation of *sil* system genes, as the wild-type B196 did not respond as strongly to the presence of exogenous SilCR as the *silCR* and *silED* knockouts.

Unlike the *sil* system in GAS, the *sil* system in SAG appears to lack *silC*, and additionally has a separate promoter upstream of *silCR*; however, data suggests that this promoter may be an internal promoter driving the transcription of *silCR*, and that *silCR* and *silED* may be part of the same operon. Future work should be done to confirm whether this is the case. If so, then examining expression through reporter constructs may not be sufficient, as the reporter constructs only report the activity of a single promoter.

Additional work should be done to detect whether *silC* exists in the SAG. Although no open reading frame was detected, a promoter was detected in the correct orientation for *silC* to exist. Normal real-time RT-PCR cannot distinguish between sense and antisense transcripts, and thus other techniques should be used to distinguish between the two.

The upregulation of *silA* in response to the presence of exogenous SilCR in Δ*silCR* and Δ*silED* is of interest, as no SilA-binding site was predicted directly upstream of *silA*. Testing to see whether transcription is being driven by the *caax* promoter upstream of *silA* should be considered, as should confirming the predicted SilA-binding sites through protein-DNA interaction assays.

Also of interest is the lower magnitude of upregulation of *silA*, *silCR* and *silE* in the presence of SilCR peptide in the wild type compared to Δ*silCR* and Δ*silED*. This indicates that there may be some negative regulation built into the system that was disrupted in the knockouts. Proper complementation of the knockouts should be made to confirm that the knockouts are not interfering with any other processes in the system, and sequencing of the knockouts can be done to confirm no mutations have occurred during recombination. It would be especially interesting to see whether a complemented ΔsilCR still overexpresses *silAB* and *silED* in the presence of exogenous SilCR, as this would provide evidence towards the existence a *silC*-like transcript.

Further research should be done into the viability of B196 at multiple stages during growth, to determine whether the cells undergo autolysis, and whether this can explain the propidium iodide staining in the cultures grown in CO_2 or Tween 80.

4.6. Conclusion

The *Streptococcus* invasion locus is a quorum-sensing system associated with virulence in the genus *Streptococcus*. Functioning as a two component quorum-sensing system, the *sil* locus appears to control the expression of an associated bacteriocin locus in both Group A *Streptococcus* and the *Streptococcus* Anginosus Group (Hidalgo-Grass *et al.*, 2002; Mendonca *et al.*, 2016). The *sil*

locus in GAS is composed of six genes under the control of four promoters: *silAB*, a two component system; *silE/D/CR*, an ABC transporter and a signal peptide; and *silC*, a non-coding transcript on the opposite strand to *silCR* (Eran *et al.*, 2007). In SAG, the system lacks the *silC* gene, and a predicted SilA-binding site lies upstream of the *silCR* gene, indicating that *silCR* may be on its own operon (Mendonca *et al.*, 2016). In this study I sought to better understand the *sil* system in SAG member *S. intermedius* B196. I examined the transcription patterns of the *sil* locus, how *sil* gene knockouts affect the transcription of the remainder of the system, and the ability of exogenous SilCR to induce the transcription of the *sil* system in both its wild-type and disrupted state.

I determined that *silA* transcription precedes the transcription of *silE* and possibly *silCR*, and that the *sil* system is under autoinduction, where the disruption of any of the three operons can downregulate the transcription of the remaining operons. The addition of exogenous SilCR has very little effect on the transcription of *sil* system genes in Δ*silA*, suggesting that SilA is the response regulator that is activated by the presence of SilCR. Exogenous SilCR can rescue transcription of *silA* and *silE* in Δ*silCR* and can rescue the transcription of *silA* in Δ*silED*, but *silCR* transcription is not completely rescued in Δ*silED*, which may suggest that *silCR* transcription is partially driven by the *silED* promoter*.* Additionally, the transcription of the wild-type *sil* locus did not increase as much in the presence of exogenous SilCR compared to the Δ*silCR* and Δ*silED* knockouts,

suggesting that there may be a mechanism by which the *sil* system prevents overexpression which is disrupted in the *silCR* and *silED* knockouts.

There exists a predicted promoter on the antisense strand of *silCR*, at approximately the same location as *silC* in the GAS. This may suggest that *silC* is present in the *sil* system of SAG, and may play a role in the negative regulation suggested above.

All three of operons of the *sil* system are required for the inhibition of SAG member *S. constellatus* M505, and that exogenous SilCR can rescue the inhibition in the *silCR* knockout, but not in either Δ*silAB* or Δ*silED*. This supports the hypothesis that *silAB* is required to respond to the presence of exogenous SilCR. Furthermore, the inability of exogenous SilCR to rescue the inhibition in Δ*silED* suggests that SilDE may be responsible for exporting and/or processing the bacteriocins required to inhibit the growth of *S. constellatus* M505.

To summarize, I was able to collect new information into the functioning of the *sil* system in *S. intermedius* B196, and compared that information to the functioning of the *sil* system in GAS. Although I have gathered evidence into the function of the autoinduction loop of the *sil* system, further research is needed to confirm the complete workings of the SAG *sil* system.

References

Abisado, R. G., Benomar, S., Klaus, J. R., Dandekar, A. A., & Chandler, J. R. (2018). Bacterial quorum sensing and microbial community interactions. *mBio*., 9(3): e02331-17.

Billroth, T. (1874). *Untersuchungen über die Vegetationsformen von Coccobacteria septica und der Antheil, welchen sie an der Entstehung und Verbreitung der accidentellen Wundkrankheiten haben*. Berlin: G. Reimer.

Behr, S., Heermann, R., & Jung, K. (2016). Insights into the DNA-binding mechanism of a LytTR-type transcription regulator. *Bioscience Reports*, 36(2): e00326.

Belotserkovsky, I., Baruch, M., Peer, A., Dov, E., Ravins, M., Mishalian, I., Persky, M., Smith, Y., & Hanski, E. (2009). Functional analysis of the quorum-sensing streptococcal invasion locus (*sil*). *PLoS Pathogens*, 5(11): e1000651.

Boratyn, G. M., Camacho, C., Cooper, P. S., Coulouris, G., Fong, A., Ma, N., Madden, T. L., Matten, W. T., McGinnis, S. D., Merezhuk, Y., Raytselis, Y., Sayers, E. W., Tao, T., Ye, J., & Zaretskaya, I. (2013). BLAST: a more efficient report with usability improvements. *Nucleic Acids Research*, 41(W1): W29–W33.

Bourret, R. B., & Silversmith, R. E. (2010). Two-component signal transduction. *Current Opinion in Microbiology*, 13(2): 113–115.

Brown, J. H. (1919). *The use of blood agar for the study of streptococci* (Vol. Monograph No. 9). New York: The Rockefeller Institute for Medical Research.

Datsenko, K. A., & Wanner, B. L. (2000). One-Step inactivation of chromosomal genes in *Escherichia coli* K-12 using PCR products. *Proceedings of the National Academy of Sciences of the United States of America*, 97(12): 6640-5.

Deibel, R. H., & Niven, C. F. (1955). The "minute" streptococci: further studies on their nutritional requirements and growth characteristics on blood agar. *Journal of Bacteriology*, 70(2): 141-146

Eran, Y., Getter, Y., Baruch, M., Belotserkovsky, I., Padalon, G., Mishalian, I., Podbielski, A., Kreikemeyer, B., & Hanski, E. (2007). Transcriptional regulation of the *sil* locus by the SilCR signalling peptide and its implications on group A streptococcus virulence. *Molecular Microbiology*, 63(4): 1209-22.

Evans, K., Stone, V., Chen, L., Ge, X., & Xu, P. (2014). Systematic study of genes influencing cellular chain length in *Streptococus sanguinis*. *Microbiology*, 160(Pt 2): 307-315.

Ferretti, J., & Köhler, W. (2016). *Streptococcus pyogenes : Basic Biology to Clinical Manifestations.* Oklahoma City, OK: University of Oklahoma Health Sciences Center.

Galperin, M. Y. (2006). Structural classification of bacterial response regulators: diversity of output domains and domain combinations. *Journal of Bacteriology*, 188(12): 4169-4182.

Gao, X., Zhi, X., Li, H., Klenk, H., & Li, W. (2014). Comparative genomics of the bacterial genus *Streptococcus* illuminates evolutionary implications of species groups. *PloS One,* 9(6): e101229.

Gossling, J. (1988). Occurence and pathogenicity of the *Streptococcus* Milleri group. *Reviews of Infectious Diseases*, 10: 257-285

Graham, M. R., Smoot, L. M., Lux Migliaccio, C. A., Virtaneva, K., Sturdevant, D. E., Porcella, S. F., Federle, M. J., Adams, G. J., Scott, J., R., & Musser, J. M. (2002). Virulence control in group A *Streptococcus* by a two-component gene regulatory system: Global expression profiling and *in vivo* infection modeling. *Proceedings of the National Academy of Science of the United States of America*, 99(21): 13855–13860.

Naville, M., Ghuillot-Gaudeffory, A., Marchais, A., & Gautheret, D. (2011). ARNold: a web tool for the prediction of Rho-independent transcription terminators. *RNA Biology,* 8(1): 11-3

Hao, N., Palmer, A. C., Dodd, I. B., & Shearwin, K. E. (2017). Directing traffic on DNA—How transcription factors relieve or induce transcriptional interference. *Transcription,* 8(2): 120–125.

Hardie, J. M., & Whiley, R. A. (1997). Classification and overview of the genera *Streptococcus* and *Enterococcus*. *Journal of Applied Microbiology Symposium* Series, 26: 1S-11S

Hidalgo-Grass, C., Ravins, M., Dan-Goor, M., Jaffe, J., Moses, A. E., & Hanski, E. (2002). A locus of group A *Streptococcus* involved in invasive disease and DNA transfer. *Molecular Microbiology,* 46(1): 87-99.

Hidalgo-Grass, C., Dan-Goor, M., Maly, A., Eran, Y., Kwinn, L. A., Nizet, V., Ravins, M., Jaffe, J., Peyser, A., Moses, A. E., & Hanski, E. (2004). Effect of a bacterial pheromone peptide on host chemokine degradation in group A streptococcal necrotising soft-tissue infections. *Lancet,* 363(9410): 696-703.

Hidalgo-Grass, C., Mishalian, I., Dan-Goor, M., Belotserkovsky, I., Eran, Y., Nizet, V., Peled, A., & Hanski, E. (2006). A streptococcal protease that degrades CXC chemokines and impairs bacterial clearance from infected tissues. *EMBO Journal,* 25(19): 4628-37.

Holm, S. (1979). A simple sequentially rejective multiple test procedure. *Scandinavian Journal of Statistics*, 6(2): 65-70.

Hook-Barnard, I. G., & Hinton, D. M. (2007). Transcription initiation by mix and match elements: flexibility for polymerase binding to bacterial promoters. *Gene Regulation and Systems Biology,* 1: 275-93

Kaiser, J. C., Verschoor, C. P., Surette, M. G., & Bowdish, D. M. (2014). Host cytokine responses distinguish invasive from airway isolates of the *Streptococcus* Milleri/Anginosis group. *BMC Infectious Diseases*, 14: 498.

Kawamura, Y., Hou, X., Sultana, F., Miura, H., & Ezaki, T. (1995). Determination of 16S rRNA sequences of *Streptococcus mitis* and *Streptococcus gordonii* and phylogenetic relationships among members of the genus *Streptococcus*. *International Journal of Systematic Bacteriology*, 45(4): 882-882.

Kirchhoff, C., & Cypionka, H. (2017). Propidium ion enters viable cells with high membrane potential during live-dead staining. *Journal of Microbiological Methods*, 142: 79-82.

Kozera, B., & Rapacz, M. (2013). Reference genes in real-time PCR. *Journal of Applied Genetics,* 54(4): 391–406.

Lacroix, AM. (2014). Investigation into competence heterogeneity in Streptococcus Milleri Group clinical isolates (Master's Thesis). Retrieved from http://hdl.handle.net/11375/14246

Laub, M. T., & Goulian, M. (2007). Specificity in two-component signal transduction pathways. *Annual Review of Genetics,* 41, 121-145.

Lancefield, R. C. (1933). A serological differentiation of human and other groups of hemolytic streptococci. *Journal of Experimental Medicine,* 57(4): 571-595.

LeBlanc, D. J., Lee, L. N., & Abu-Al-Jaibat, A. (1992). Molecular, genetic, and functional analysis of the basic replicon of pVA380-1, a plasmid of oral streptococcal origin. *Plasmid*, 28(2): 130-45.

Lyon, G. J., & Novick, R. P. (2004). Peptide signaling in *Staphylococcus aureus* and other Gram-positive bacteria. *Peptides,* 25(9): 1389-403.

Mendonca, M. L., Szamosi, J. C., Lacroix, A. M., Fontes, M. E., Bowdish, D. M., & Surette, M. G. (2016). The *sil* locus in *Streptococcus* Anginosus Group: interspecies competition and a hotspot of genetic diversity. *Frontiers in Microbiology*, 7: 2156.

Mellroth, P., Daniels, R., Eberhardt, A., Rönnlund, D., Blom, H., Widengren, J., & Henriques-Normark, B. (2012). LytA, major autolysin of *Streptococcus pneumoniae*, requires access to nascent peptidoglycan. *Journal of Biological Chemistry,* 287(14): 11018-11029.

Michael-Gayego, A., Dan-Goor, M., Jaffe, J., Hidalgo-Grass, C., & Moses, A. E. (2013). Characterization of *sil* in invasive group A and G streptococci: antibodies against bacterial pheromone peptide SilCR result in severe infection. *Infection and Immunity*, 81(11): 4121-7.

Nielsen, C. K., Kjems, J., Mygind, T., Snabe, T., & Meyer, R. L. (2016). Effects of Tween 80 on growth and biofilm formation in laboratory media. *Frontiers in Microbiology*, 7: 1878.

Olson, A. B., Kent, H., Sibley, C. D., Grinwis, M. E., Mabon, P., Ouellette, C, Tyson, S., Graham, M., Tyler, S. D., Van Domselaar, G., Surette, M. G., & Corbett, C. R. (2013). Phylogenetic relationship and virulence inference of Streptococcus Anginosus Group: Curated annotation and whole-genome comparative analysis support distinct species designation. *BMC Genomics*, 14(1): 895.

Opdyke, J. A., Scott, J. R., & Morgan Jr., C. P. (2003). Expression of the secondary sigma factor σ^X in *Streptococcus pyogenes* is restricted at two levels. *Journal of Bacteriology,* 185(15): 4291–4297.

Piscitelli, S. C., Shwed, J., Schreckenberger, P., & Danziger, L. H. (1992). *Streptococcus* Milleri group: renewed interest in an elusive pathogen. *European Journal of Clinical Microbiology and Infectious Disease*, 11: 491-498

Plainvert, C., Dinis, M., Ravins, M., Hanski, E., Touak, G., Dmytruk, N., Fouet, A., & Poyart, C. (2014). Molecular epidemiology of *sil l*ocus in clinical *Streptococcus pyogenes s*trains. *Journal of Clinical Microbiology*, 52(6): 2003–2010.

Pulliam, L., Porschen, R. K., & Hadley, W. K. (1980). Biochemical properties of CO2-dependent streptococci. *Journal of Clinical Microbiology*, 12(1): 27-31.

Solovyev, A., & Salamov, A. (2011). Automatic annotation of microbial genomes and metagenomic sequences. In Li, R. W. (Eds.), *Metagenomics and its Applications in Agriculture, Biomedicine and Environmental Studies* (p. 61-*7*8). Hauppage*,* NY: Nova Science Publishers.

Raivio, T. L., & Silhavy, T. J. (1997). Transduction of envelope stress in *Escherichia coli* by the Cpx two-component system. *Journal of Bacteriology*, 179(24): 7724-33.

Ruoff, K. L. (1988). *Streptococcus anginosus* ("*Streptococcus milleri*"): The unrecognized pathogen. *Clinical Microbiology Reviews*, 1(1): 102-108.

Salim, K. Y., de Azavedo, J. C., Bast, D. J., & Cvitkovitch, D. G. (2008). Regulation of *sagA*, *siaA* and *scpC* by SilCR, a putative signaling peptide of *Streptococcus pyogenes*. *FEMS Microbiology Letters*, 289(2): 119-25.

Schleifer, K., & Kilpper-Bälz, R. (1987). Molecular and chemotaxonomic approaches to the classification of streptococci, enterococci and lactococci: a review. *Systematic and Applied Microbiology,* 10(1): 1-19.

Sherman, J. M. (1937) The streptococci. *Bacteriological Reviews,* 1: 3–97

Shi, L., Günther, S., Hübschmann, T., Wick, L. Y., Harms, H., & Müller, S. (2007). Limits of propidium iodide as a cell viability indicator for environmental bacteria. *Cytometry Part A*, 71A(8): 592-598.

Siegman-Igra, Y., Azmon, Y., & Schwartz, D. (2012). Milleri group streptococcus--a stepchild in the viridans family. *European Journal of Clinical Microbiology & Infectious Diseases*, 31(9): 2453-9.

Steinmoen, H., Knutsen, E., Håvarstein, L. S. (2002). Induction of natural competence in *Streptococcus pneumoniae* triggers lysis and DNA release from a subfraction of the cell population. *Proceedings of the National Academy of Sciences of the United States of America,* 99(11): 7681–7686.

Stevenson, K., McVey, A. F., Clark, I. B. N., Swain, P. S., & Pilizota, T. (2016). General calibration of microbial growth in microplate readers. *Scientific Reports*, 6: 38828

Stocks, S.M. (2003). Mechanism and use of the commercially available viability stain, *Bac*Light. *Cytometry,* 61A(2): 189-195.

Stoll, S., Feldhaar, H., & Gross, R. (2009). Promoter characterization in the AT-rich genome of the obligate endosymbiont "*Candidatus* Blochmannia floridanus". *Journal of Bacteriology,* 191(11): 3747-51.

Wang, C. Y., Patel, N., Wholey, W. Y., & Dawid, S. (2018). ABC transporter content diversity in *Streptococcus pneumoniae* impacts competence regulation and bacteriocin production. *Proceedings of the National Academy of Sciences of the United States of America,* 115(25): E5776–E5785.

Washburn, R. S., Marra, A., Bryant, A. P., Rosenberg, M., & Gentry, D. R. (2001). *rho* is not essential for viability or virulence in *Staphylococcus aureus*. *Antimicrobial Agents and Chemotherapeutics*, 45(4): 1099–1103.

Wen, S., Chen, X., Xu, F., & Sun, H. (2016). Validation of reference genes for real-time quantitative PCR (qPCR) analysis of *Avibacterium paragallinarum*. *PLoS One*, 11(12): e0167736.

West, A. H., & Stock, A. M. (2001). Histidine kinases and response regulator proteins in two-component signaling systems. *Trends in Biochemical Sciences,* 26(6): 369-76.

Wisniewski-Dyé, F., & Boyer, M. (2009). Cell–cell signalling in bacteria: not simply a matter of quorum. *FEMS Microbiology Ecology,* 70(1): 1-19.